ELSEVIER

Journal of Marine Systems 20 (1999) 129–156

JOURNAL OF MARINE SYSTEMS

The Atlantic Ionian Stream

A.R. Robinson [a,*], J. Sellschopp [b], A. Warn-Varnas [c], W.G. Leslie [a], C.J. Lozano [a], P.J. Haley Jr. [a], L.A. Anderson [a], P.F.J. Lermusiaux [a]

[a] *Harvard University, Division of Applied Sciences, Department of Earth and Planetary Sciences, 29 Oxford Street, Cambridge, MA, USA*
[b] *SACLANT Undersea Research Centre, La Spezia, Italy*
[c] *Naval Research Laboratory, Stennis Space Center, MS, USA*

Received 1 February 1997; accepted 18 June 1998

Abstract

This paper describes some preliminary results of the cooperative effort between SACLANT Undersea Research Centre and Harvard University in the development of a regional descriptive and predictive capability for the Strait of Sicily. The aims of the work have been to: (1) determine and describe the underlying dynamics of the region; and, (2) rapidly assess synoptic oceanographic conditions through measurements and modeling. Based on the 1994–1996 surveys, a picture of some semi-permanent features which occur in the Strait of Sicily is beginning to emerge. Dynamical circulation studies, with assimilated data from the surveys, indicate the presence of an Adventure Bank Vortex (ABV), Maltese Channel Crest (MCC), and Ionian Shelf Break Vortex (IBV). A schematic water mass model has been developed for the region. Results from the Rapid Response 96 real-time numerical modeling experiments are presented and evaluated. A newly developed data assimilation methodology, Error Subspace Statistical Estimation (ESSE) is introduced. The ideal Error Subspace spans and tracks the scales and processes where the dominant, most energetic, errors occur, making this methodology especially useful in real-time adaptive sampling.

Keywords: Atlantic Ionian Stream; Strait of Sicily; Error Subspace Statistical Estimation

1. Introduction

In 1994, the SACLANT Undersea Research Centre and Harvard University began the development of a regional descriptive and predictive capability for the Strait of Sicily. The aims of the work have been to: (1) determine and describe the underlying dynamics of the region; and, (2) rapidly assess synoptic oceanographic conditions through measurements and modeling. Our cooperative cruises have provided synoptic data to define the structures present. This work builds on previous work in the region, including that of Grancini and Michelato (1987).

The development of a predictive capability for the Strait of Sicily region has evolved through three phases (Robinson et al., 1996). Those three phases are: exploratory, dynamical, and predictive. The exploratory phase is descriptive and kinematic and

* Corresponding author. Fax: +1-617-495-5192; E-mail: robinson@pacific.harvard.edu

0924-7963/99/$ - see front matter
PII: S0924-7963(98)00079-7

involves the identification of regional scales, phenomena, processes and interactions. The dynamical phase defines synoptic flow structures, regional synoptical dynamical events and interactions, and elucidates dynamical processes governing mesoscale evolution and sub-mesoscale events. The predictive phase involves predictive experiments and the design of an efficient regional forecast system with minimum resources for desired accuracy and applications. Forecast experiments have been performed with high quality data sets and have described the regional circulation, dynamics, variabilities, exchanges, and interactions. Dedicated cruises have taken place in 1994, 1995 and 1996. During each cruise, data was assimilated in real-time, at sea, as it became available. Adaptive sampling, based on shipboard predictions, was used to investigate potentially interesting phenomena.

In the Strait of Sicily, the fresh Atlantic inflow and the salty Levantine outflow constitute a two-current system of the general circulation of the Mediterranean. The Levantine outflow is located at depth and the Atlantic inflow is in the upper ocean. The Atlantic water enters into the Mediterranean through the Strait of Gibraltar as an inflowing jet in the surface layer of the Alboran Sea. It then becomes the Algerian current along the North African coast and arrives at the Strait of Sicily, where it marks the

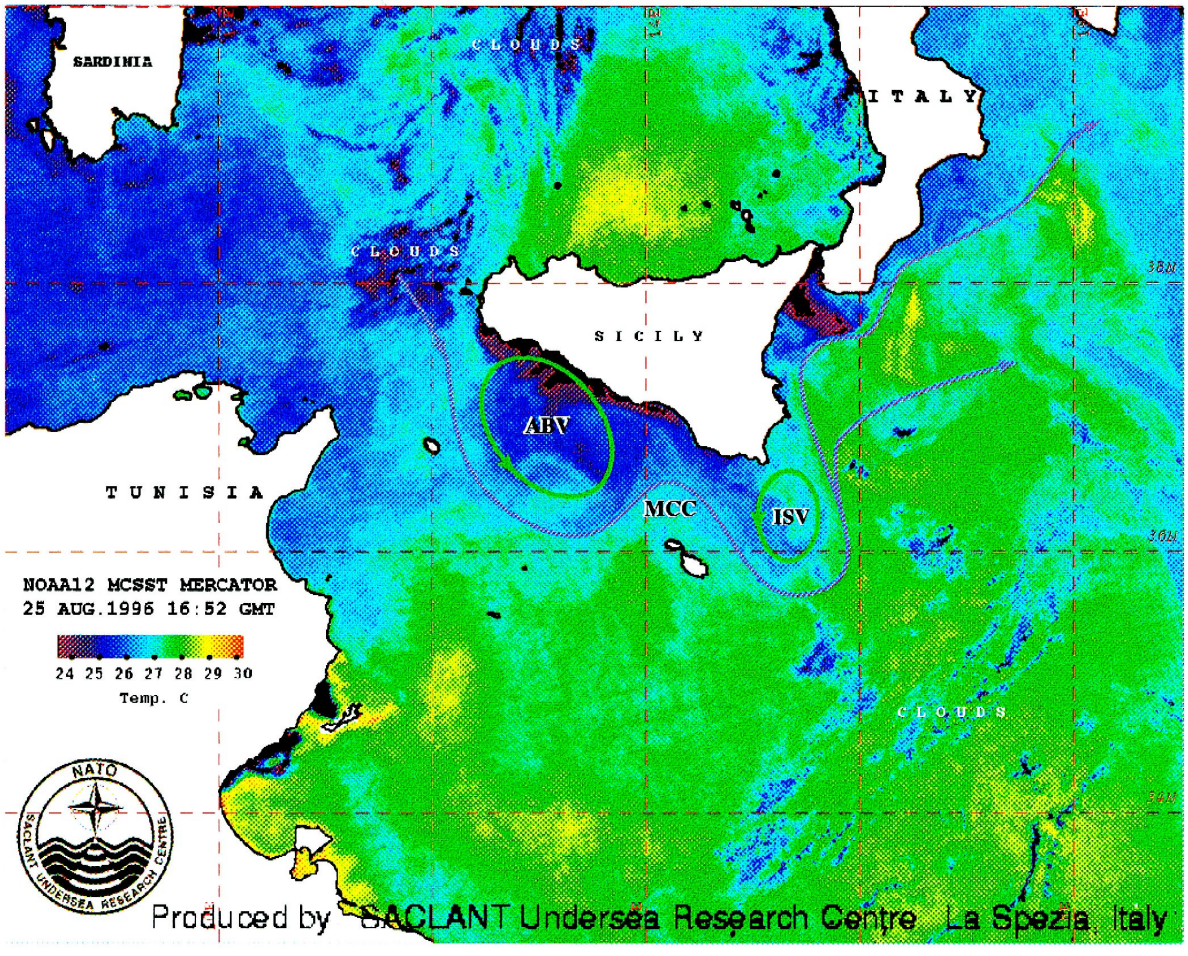

Fig. 1. Sea surface temperature on 25 August 1996 with a schematic of important circulation structures superimposed.

beginning of the Atlantic Ionian Stream (AIS) (Robinson et al., 1991), flows past Malta and turns northward where, we believe, it was first identified as a local feature over the shelf break, i.e., the Maltese Front (Johannessen et al., 1977). Subsequently, the AIS flows off the shelf into the upper, western Ionian Sea, with an intense looping northward meander, which generally decreases in amplitude during the winter. Various analyses of data gathered in this region (Grancini and Michelato, 1987; Moretti et al., 1993; Manzella et al., 1990) have described the Atlantic inflow as having a filamented but predominantly two-jet structure spanning the upper 100 m, with an associated salinity minimum, flowing closest to Tunisia and along the coast. The two-jet structure has not been observed, though, during the AIS investigations. Bifurcations of the AIS develop, with southerly branches, in the Strait of Sicily and Ionian Sea. This region contains a number of significant processes and phenomena. In addition to the general circulation with its mesoscale variability, there are the wind-driven currents on the shelf from local and remote storms (including the Sicilian coastal current) and upwelling off Sicily. Tides, inertial, gravity, surface, and continental shelf waves occur. This region contains active water mass modification processes between the fresher and warmer water mass of Atlantic origin and the saltier and colder Levantine water mass.

A picture of some semi-permanent features which occur in the Strait of Sicily is beginning to emerge; based on the AIS-94, 95, and 96 surveys. Dynamical circulation studies, with assimilated data from the surveys, indicate the presence of an Adventure Bank Vortex (ABV), Maltese Channel Crest (MCC), and Ionian Shelf Break Vortex (IBV). These are part of the AIS circulation structure in the Strait of Sicily. Fig. 1 shows a sketch of these features superimposed on a satellite SST distribution for 25 August 1996.

Some water mass analysis has previously been performed in the Strait of Sicily region in conjunction with Physical Oceanography of the Eastern Mediterranean (POEM) September 1987 survey. Theocharis et al. (1993) have analyzed the summer 1987 data in the Ionian Sea and have derived five water masses. The surface layer, the top 100 m, was characterized as surface Ionian water with Atlantic water below. Below that there were Levantine, Transition, and Deep waters. Our analysis will break down these categories further, using information from the more intensive surveys of the Strait of Sicily region. A recent analysis of water masses in the Ionian from POEM data can be found in Malanotte-Rizzoli et al. (1997).

The paper is organized into sections on data description, circulation and water mass studies, variabilities and prediction, and summary and conclusion.

2. Data sets

This data section has been separated into three sections which describe the data collected during the dedicated SACLANTCEN/Harvard surveys of 1994, 1995 and 1996. The hydrography, direct current measurements (current meter and ADCP), and drifter data will be presented separately. Within each subsection, the data will be presented by year. The data is not interpreted here; it is only described as to its location and methodology.

2.1. Hydrographic data

2.1.1. AIS94

The AIS-94 (November 1994) survey was conducted along the southern and southeastern Sicilian coasts. The plan consisted of a mesoscale resolution survey of the large region extending from Trapani (at the western tip of Sicily) to the southeastern coast and into the western Ionian Sea. Embedded within this survey was a fine-resolution survey along the shelfbreak (Fig. 2a). The data consisted of CTD's (53), XCTD's (102), and XBT's (138). The spacing along tracks, for the large scale survey, was approximately 14 km and the distance between adjacent tracks 35 km. For the fine scale survey of the shelfbreak, a spacing of 7 km was used between stations and tracks.

2.1.2. AIS95

AIS-95 (October 1995) provided a more thorough coverage of the large scale structure of the Strait (Fig. 2b). The tracks again began at the western coast of Sicily and proceeded to the southeastern shelfbreak with a spacing of 18.5 km between hydro-

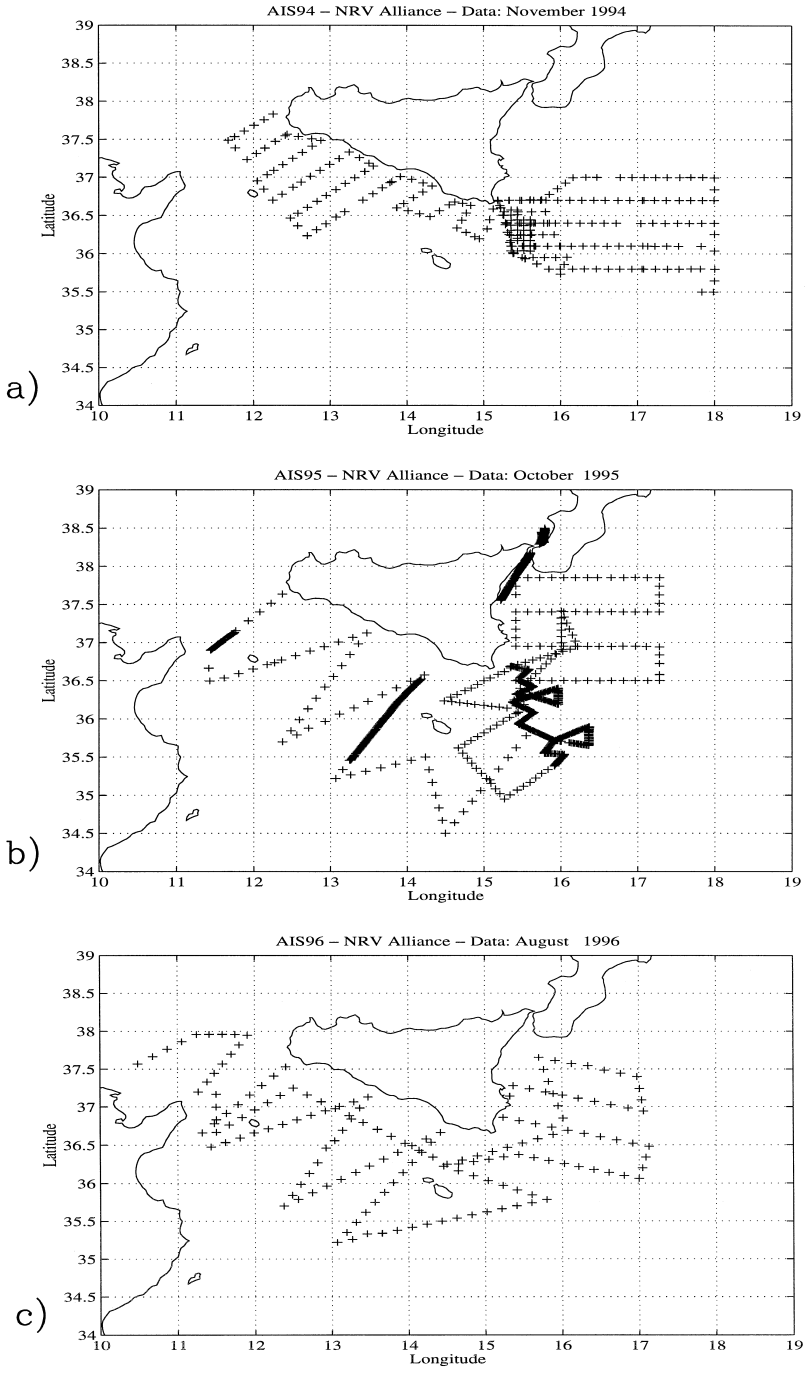

Fig. 2. Positions of hydrographic observations; (a) AIS94, (b) AIS95, (c) AIS96.

casts. After the deployment of moorings on the shelfbreak, tracks into the Ionian Sea were carried out (with a spacing of 9.25 km between hydrocasts) for the purpose of locating the looping of the AIS expected there. Subsequently, a shelfbreak survey was performed, with a spacing of 13.9 km, along the

Table 1
AIS-94 moorings (10 min. averaging on all instruments)

Number	Location	Type	Depth (m)
A (M3)	36°15.22′N,	AANDERA	450
	15°23.42′E	ADCP 75 kHz	450
		28 BINS OF 16 m	
B (M2)	36°24.09′N,	AANDERAA	85
	15°28.55′E	AANDERAA	254
		AANDERAA	484
C (M4)	36°06.16′N,	AANDERAA	41
	15°26.21′E	AANDERAA	204
		AANDERAA	411

shelf region that had not yet been surveyed. From the northern end of these tracks, a rectangular survey of the northwest Ionian Sea was conducted. A total of 96 CTD, 41 XCTD and 82 XBT stations were collected. In addition to the standard hydrographical probes, a CTD chain had been constructed and was used along selected portions of the tracks for measuring temperatures and salinities on scales down to the order of meters in the upper ocean. This enabled the description of extremely small scales, together with the mesoscale. The chain deployments were focused on regions where the presence of the AIS was anticipated. Horizontal and vertical resolutions were about 5 m and 2.5 m, respectively. The thick black lines in Fig. 2b indicates the locations of the CTD chain deployment.

2.1.3. AIS96

As in previous cruises, the AIS-96 (August 1996) tracks began at the western coast of Sicily and proceeded to the southeastern shelfbreak (Fig. 2c). The western Ionian was surveyed next, from south to north. Ship-board modeling results, which indicated areas in which sampling would be most beneficial, helped to determine the return track to the mouth of the Strait. Nominal along-track spacing was 15 km. In addition to CTD (77), XCTD (45), and XBT (46) stations, AXBT drops (not shown) were conducted on August 12, 15, 17, 19, and 24. The AXBT flight plans were developed at-sea based on ship-board predictions.

2.2. Direct velocity data

2.2.1. AIS94

Moorings were deployed along the shelfbreak near the vicinity of the 600 m depth. Their location encompassed the region where the Maltese front had previously been observed (Johannessen et al., 1977) (Fig. 3a). They consisted of an ADCP deployed at the central location, at about 450 m from the surface, and two regular moorings with three-Aanderaa current meters on each. The specifications are given in Table 1. The ship's ADCP (75 kHz) monitored the ocean currents along the tracks of the survey. It was configured to measure the upper ocean region with 20 cells of 8 m thickness and a 5 min averaging interval.

2.2.2. AIS95

Moorings were deployed on the southeastern shelfbreak in the same general location as in AIS-94 (Fig. 3b). They were left on location, beyond the time span of the hydrographic experiment; until December 15, 1995. Four moorings were configured with Aanderaa current meters (Table 2). The AIS was monitored by each mooring with one current meter located in its expected layer thickness. Other meters tracked the surface and transition to Levantine water layers. The region close to the bottom of the shelf was monitored by 1 m.

The 75 kHz shipboard ADCP was configured into 80 cells of 8 m thickness with 5 min averaging. The data was processed onboard ship with the CODAS-3 software from the University of Hawaii. As a result, it was possible to map the AIS along the tracks during the cruise. Fig. 3c exhibits the ocean currents in the layer from 50 to 70 m.

Table 2
AIS-95 moorings (20 min. averaging on all instruments)

Number	Location	Type	Depth (m)
M2	36°23.48′N,	AANDERAA	37
	15°28.50′E	AANDERAA	77
		AANDERAA	210
M3	36°14.48′N,	AANDERAA	17
	15°23.57′E	AANDERAA	59
		AANDERAA	197
		AANDERAA	564
M4	36°04.58′N,	AANDERAA	38
	15°26.52′E	AANDERAA	79
		AANDERAA	210
M5	35°56.20′N,	AANDERAA	30
	15° 28.20′E	AANDERAA	205

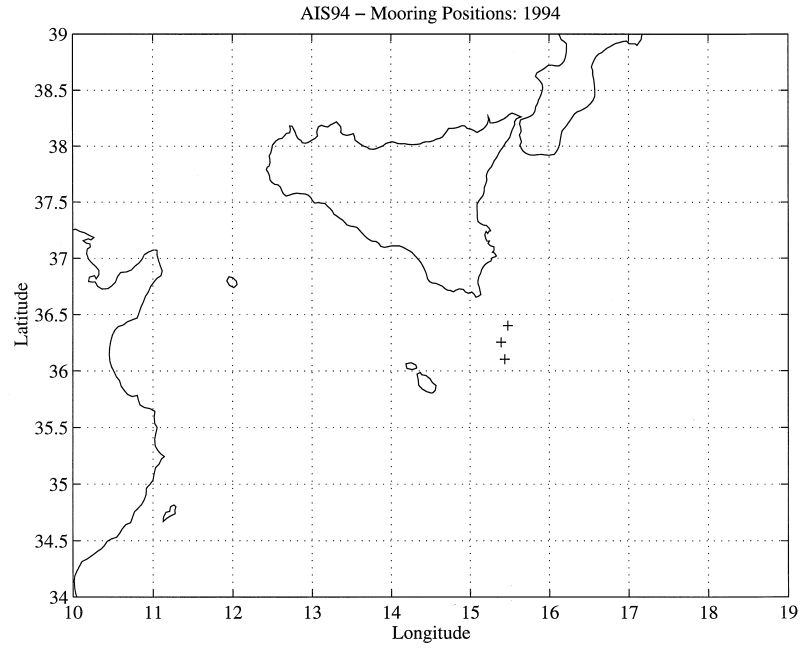

a)

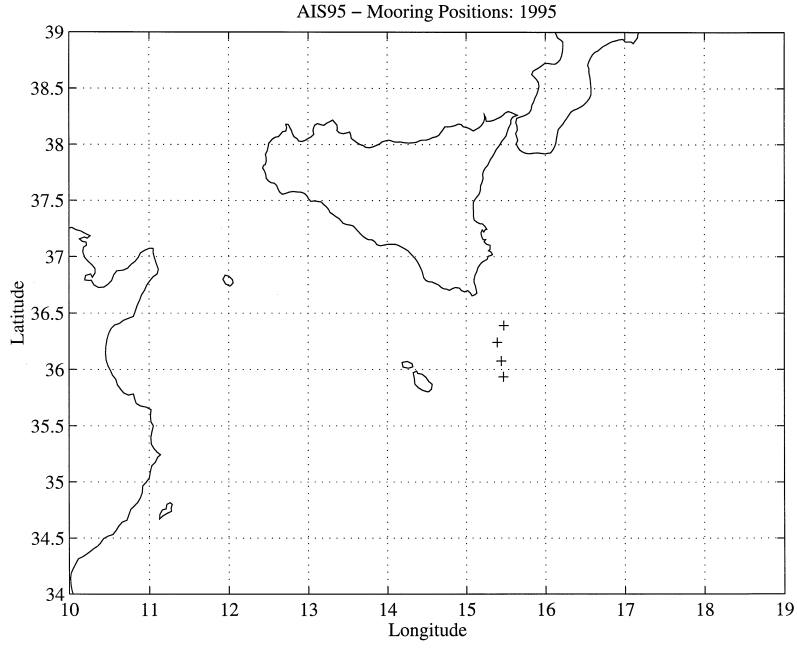

b)

Fig. 3. (a) Mooring positions—AIS94. (b) Mooring positions—AIS95. (c) Velocities in the 50–70 m layer as measured by ADCP during AIS95.

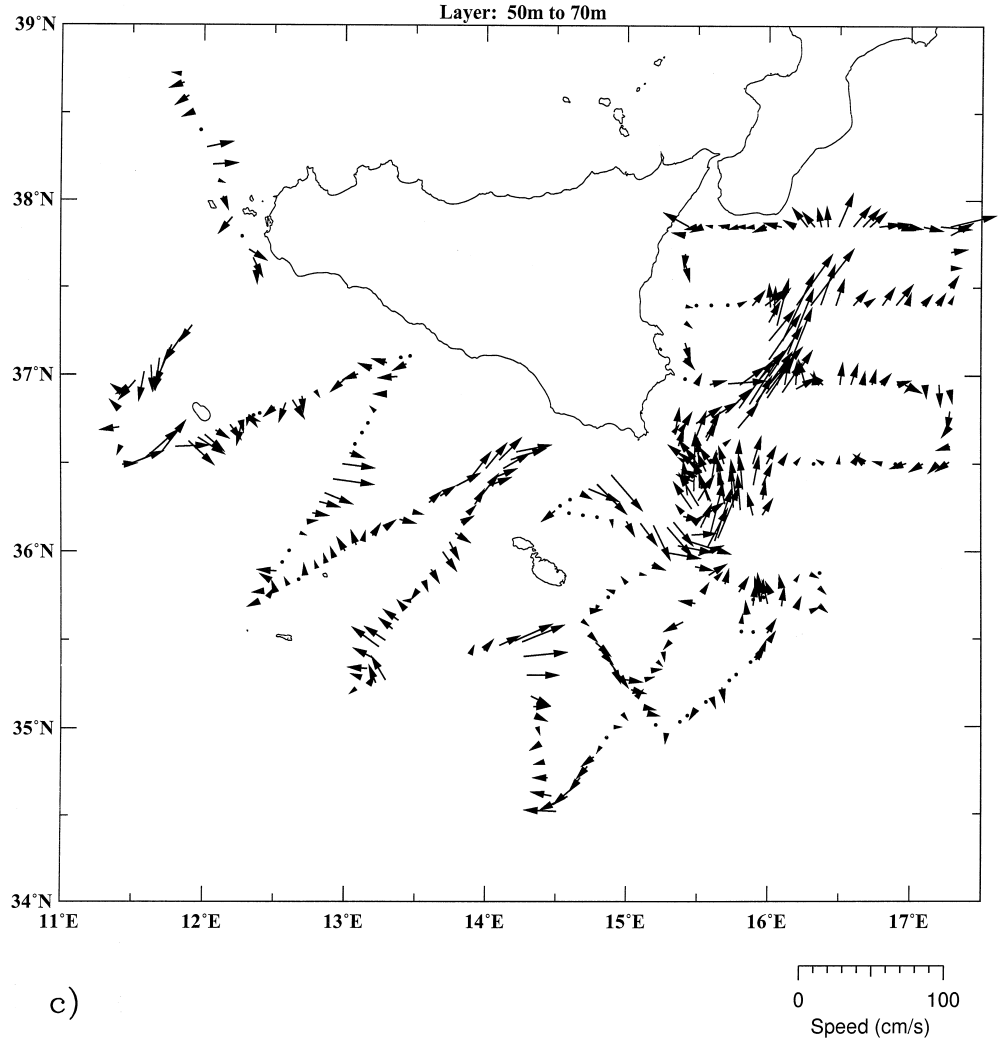

Fig. 3 (continued).

2.3. Drifter data

2.3.1. AIS94

During the November AIS-94 survey, six surface drifters were released in the vicinity of the moorings on the shelfbreak where the AIS was expected to be present. They were located on a line along longitude 15°26′E. The tracks from November 1994 to February of 1996 indicate the AIS flow (Fig. 4).

2.3.2. AIS95

In October of 1995, surface drifters were released at the western end of the Sicilian Strait, the southern region of the Strait and on the Malta shelf break region (Fig. 5). These drifters enabled the tracking of the varying flow structure in the different regions of the Strait.

3. Circulation and water masses

3.1. Circulation

The topography of the Strait of Sicily consists of shallow banks along the Sicilian and Tunisian coasts. There the water depth ranges from 50 to 200 m. The

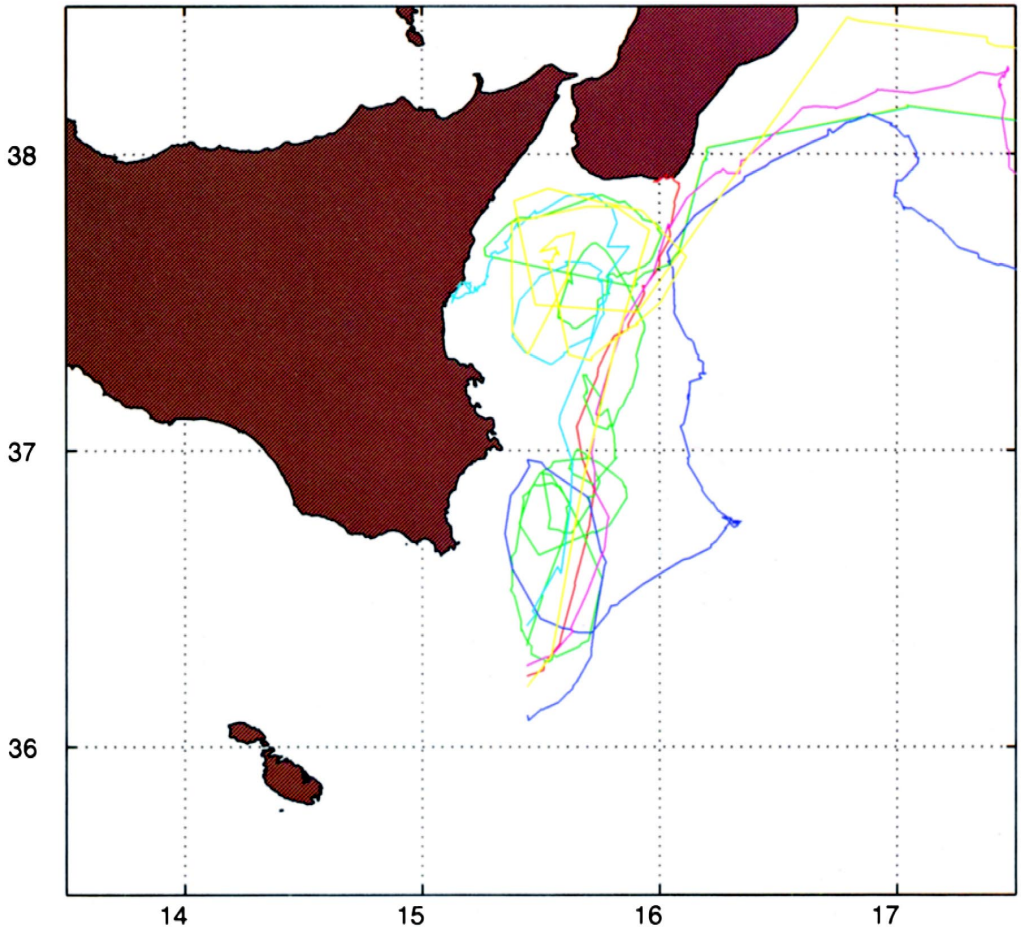

Fig. 4. Surface drifter trajectories during AIS94.

bank on the Tunisian side covers a substantial part of the surface area in the strait. Between the shallow banks deeper channels exist, with depths to around 1000 m. Proceeding southeast from Sicily the depth changes from the 50 m range to around 600 in the shelfbreak region. There a steep drop occurs, to approximately 3 km, over a short distance. Fig. 6 illustrates the topographic variability. The solid lines indicate the locations of standard vertical sections (temperature, salinity, sound speed) which were used for analysis and distribution in real time during the NATO exercise Rapid Response 96.

On the southeastern Sicilian shelfbreak, the ocean current structure was monitored with moorings during the AIS94 and 95 surveys. A preliminary analysis of the AIS-94 mooring data has been conducted. The measurements at the northern-most mooring are shown in Fig. 7. The time series at 86 m indicates a dominant presence of northeasterly flow that is part of the AIS at this depth range. The two moorings located south of this position do not show the AIS presence. At the 254 and 484 m depths, there is a notable reversal of the flow to the southerly direction. The time series structures at 86 and 254 m show variability. Objective analysis of the hydrography data taken during the three AIS-94 shelfbreak surveys, indicates rapid, mesoscale variability occurring.

The drifters released on the shelfbreak during the AIS-94 cruise (Fig. 4) moved northwards and on into the Ionian Sea. Off the Sicilian coast a vortex occurred. The flow bifurcated, with one branch de-

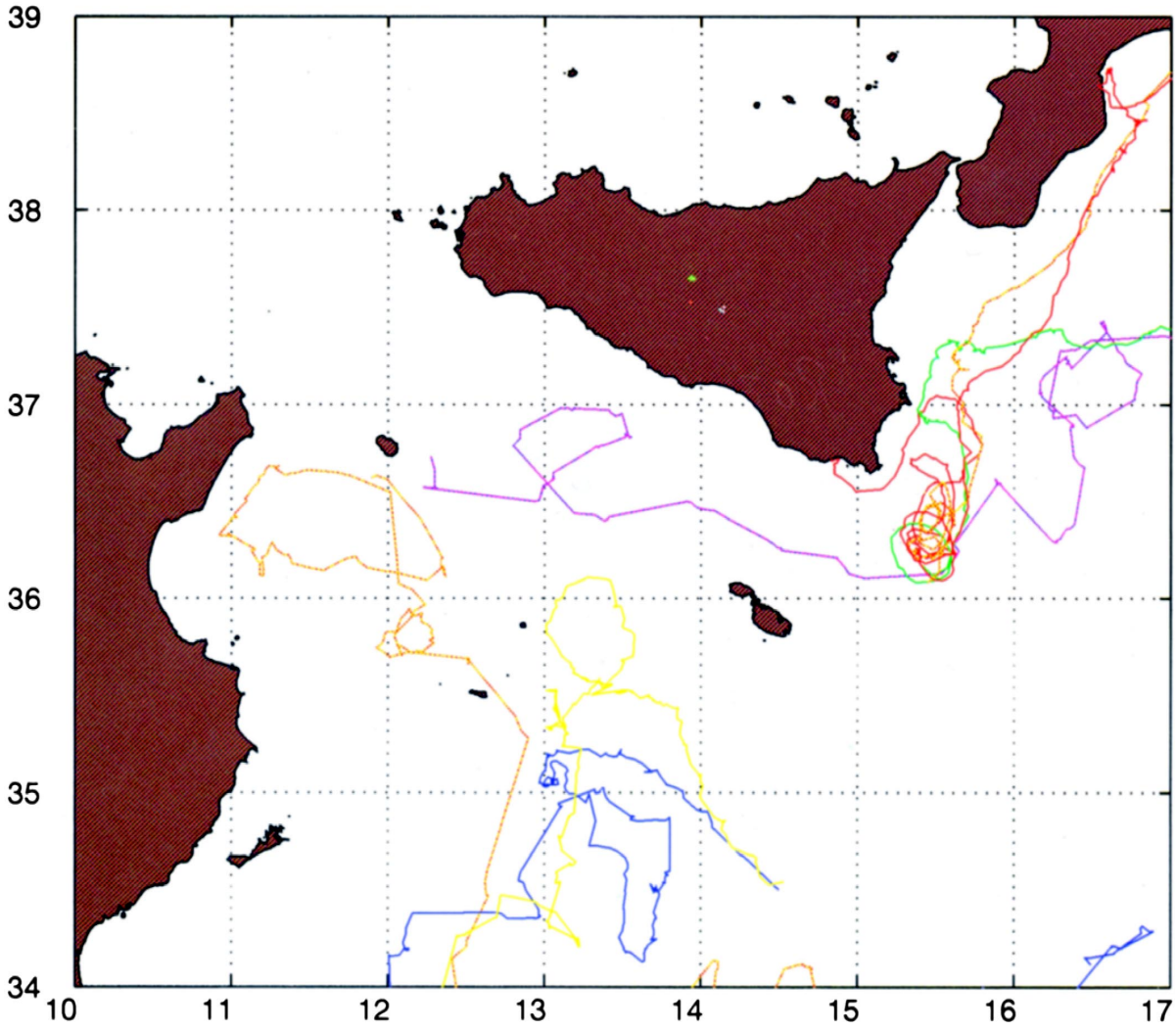

Fig. 5. Surface drifter trajectories during AIS95.

scending to the Libyan coast, outlining the Ionian Sea Anti-Cyclonic Gyre. The other branch proceeded to Peloponnisos.

For the AIS-95 data, a similar picture of upper ocean circulation exists. Fig. 3 has shown the processed ocean currents, as measured by ADCP, in the layer from 50 to 70 m along the AIS-95 cruise tracks. This depth range includes the AIS flow. The vector distribution is suggestive of a looping around the ABV and the MCC. A turning of the flow onto the shelfbreak and continuation into the Ionian Sea is evident. On the shelfbreak, a IBV could be present as part of a tracked cyclonic circulation pattern in the area. We note the segments of the captured current, from west to east, as the AIS flows along the Strait. On the shelfbreak and on into the Ionian Sea, the flow is particularly visible, due to track configuration.

Surface drifters were released throughout the AIS-95 cruise at a number of locations (Fig. 5). Two drifters were released on the eastern side of Pantelleria Island. Each was placed in what was expected to

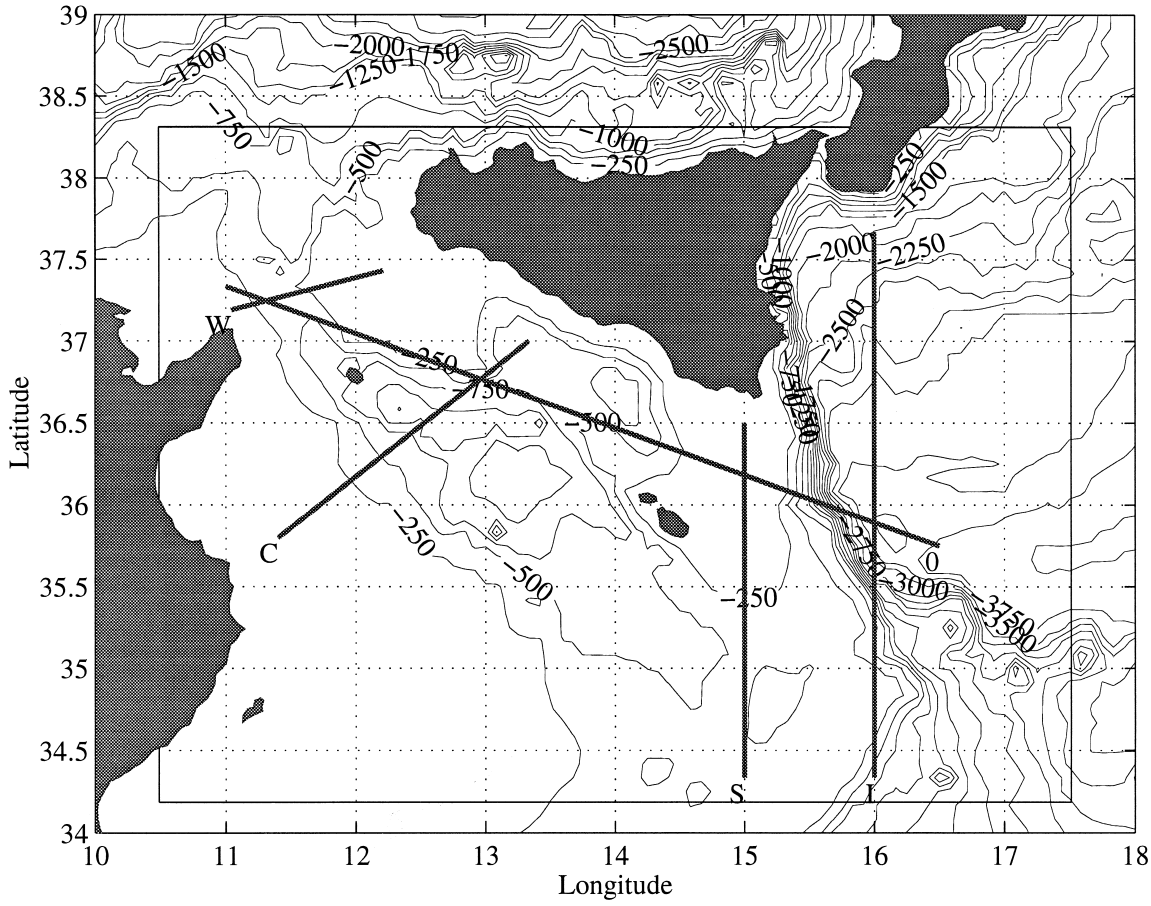

Fig. 6. Bottom topography in Strait of Sicily region (250 m contours). Also indicated is the modelling domain of AIS96 and the locations of vertical sections as provided during the Rapid Response exercise.

be a different branch of the AIS. The northern one looped around in the ABV area and went on to the shelfbreak. From there it proceeded into the Ionian Sea where it went around a anti-cyclonic vortex. The other drifter, on the southern side of Pantelleria Island, turned towards Tunisia, looped back, spent time in a cyclonic eddy, and then proceeded towards the Libyan coast.

Two other drifters were placed around 35°N, 14°E. At first they both traveled northwest together. Then their paths diverged, with one turning more westwards and proceeding south around a cyclonic vortex. The other looped around a anti-cyclonic vortex and returned to the south. Both of the tracks eventually headed south towards Libya. The drifters outlined a varying mesoscale field in the area.

On the shelfbreak, four drifters were released. They all spent time in the IBV. From there they proceeded north. One turned southwest and beached itself on the Sicilian coast. Two of the others went northeast, along the Sicilian and Italian coasts. One turned and moved straight east into the Ionian Sea.

The circulation in the region can be determined, not only from ADCP, current meter or drifter measurements, but also from a combination of synoptic data and model dynamics. Short term (a few day) model runs are used to dynamically adjust the complete data set. This is termed a dynamically adjusted nowcast, or in the case of historical simulations, a hindcast. A primitive equation dynamical model is used with a horizontal grid resolution of 9 km. A terrain-following (double-sigma) vertical coordinate

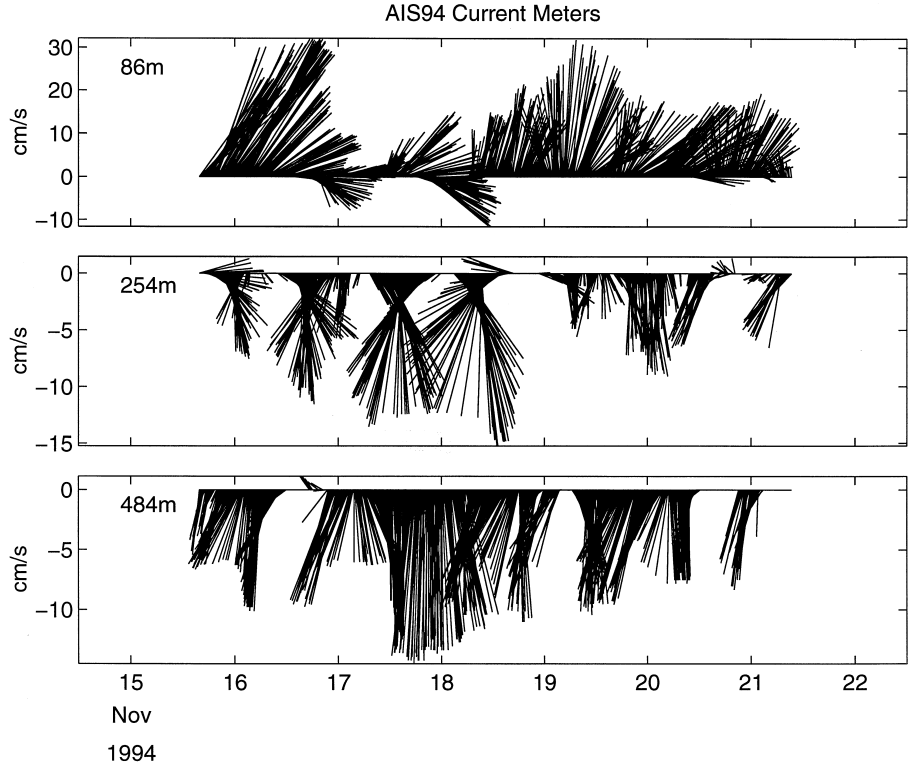

Fig. 7. Velocity measurements from the northern-most mooring during AIS94.

system is employed. Model levels 6 and 18 generally represent the near surface and core Levantine Intermediate Water (LIW) conditions, respectively. For open boundaries, the implicit Orlanski radiation condition is utilized for the transport streamfunction and internal velocities; for tracers, the condition is either fixed or radiation. At closed boundaries, a free-slip condition is applied to total velocities and a no-flux condition is imposed on tracers. Surface forcings are momentum, heat flux and evaporation-precipitation, as calculated from FNOC supplied analyses and forecasts.

The short term, 4 day, hindcast of temperature for near surface conditions shown in Fig. 8 displays the circulation associated with the measured hydrography fields for AIS-95 (October 1995). In the surface layer, the AIS enters the Strait of Sicily at the western inlet. It then meanders south around the ABV and loops back northward around Malta, forming the MCC. From there, north of Malta, another loop southward occurs around the cyclonic ISV. The flow proceeds onto the shelfbreak and on into the Ionian Sea. There the flow loops south again, generating a small anti-cyclonic gyre. Along the path of the AIS, a temperature difference of several tenths of degrees occurs from the western end to the southeastern Sicilian shelf break. Once the AIS leaves the shelf break, the temperature contrast disappears. The corresponding salinity in Fig. 9a ranges from about 37.3 to 37.7 and is indicative of Atlantic type water. In the core LIW depth in the Strait, represented by model level 18 (Fig. 9b), salinities are higher than shallower depths, with Strait salinities greater than 38.7.

A plot of model hindcasted temperature and salinity results along section O (see Fig. 6), is shown in Fig. 10 (temperature–upper panel; salinity–lower panel). The hindcast is for 4 days initialized from all of the AIS-95 data. An upper thermocline is apparent in the temperature gradients, as the surface region is approached. At the surface the warm spots are indicative of a summer situation with a near surface

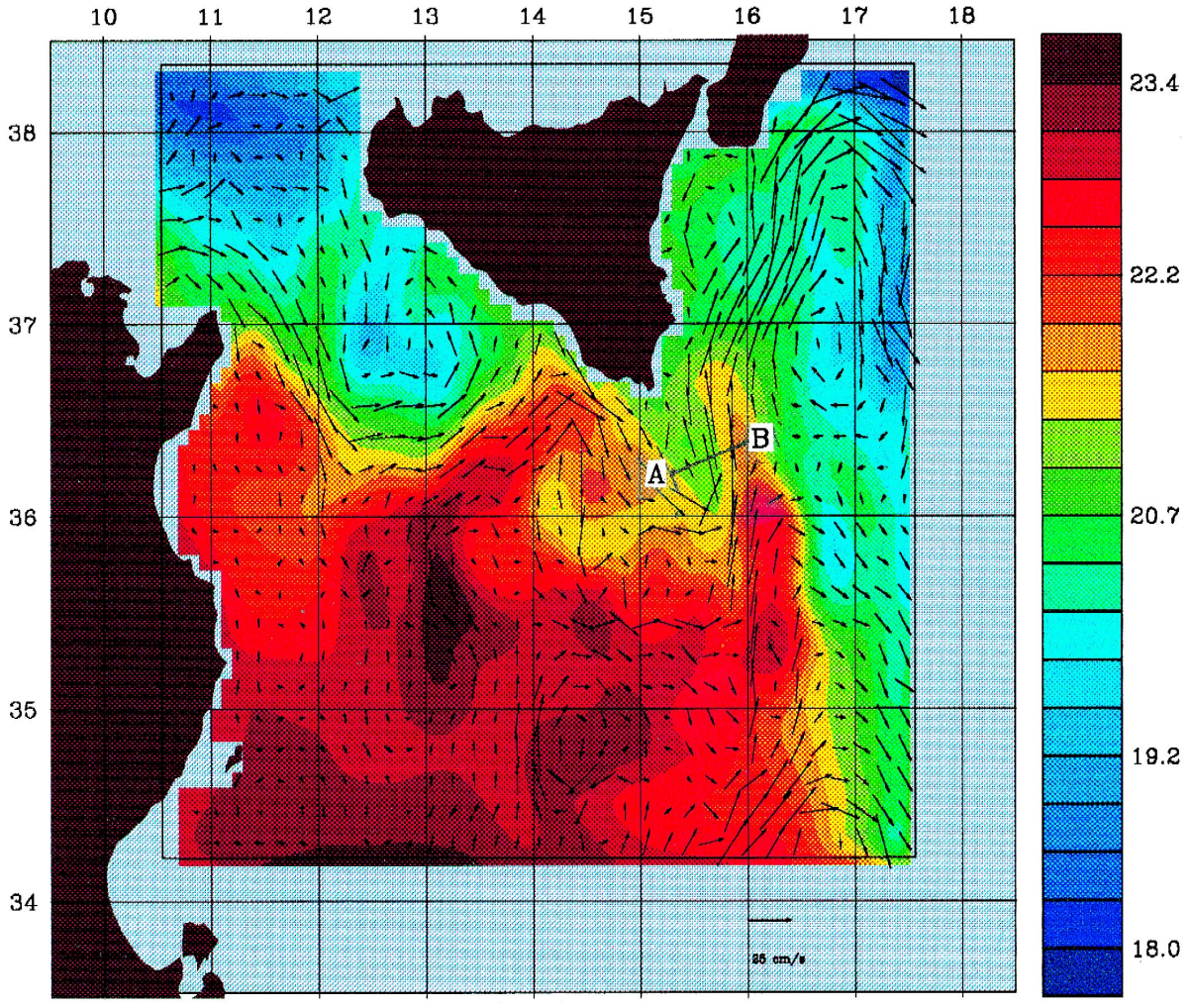

Fig. 8. Short-term hindcast of temperature for near-surface conditions during AIS95.

seasonal thermocline capped with a shallow mixed layer. The upper ocean salinity distribution contains the less saline, Atlantic (AIS) type, water along the track in the strait and shelfbreak. Off the shelfbreak and on into the Ionian Sea, the salinity increases. At a depth of 300 m there is a concentration of LIW. On the shelfbreak ridge, located around 200 m, an overflow of LIW from the Ionian is apparent. This breaks into high salinity blob structures in the strait.

CTD stations along a track, even if their spacing is smaller than the scales of the meso- and submesoscale features of interest, contain finer scale structures which can contaminate the signal. Finer scale measurements are necessary: to define the smaller scale structures, to justify the (sub) mesoscalesampling scheme and to design an adequate filtering scheme and to design an adequate filtering scheme. For example, the scale separation of features contained in sampled density profile series, and the measurement of the extension of intruded patches, can only be solved by horizontally dense measurements.

To explore the finer scales in AIS95, the towed CTD chain (Sellschopp, 1997) of FWG (Forschungsanstalt der Bundeswehr Für Wasserschall-und Geophysik, Kiel, GE) was used. The chain in the AIS95

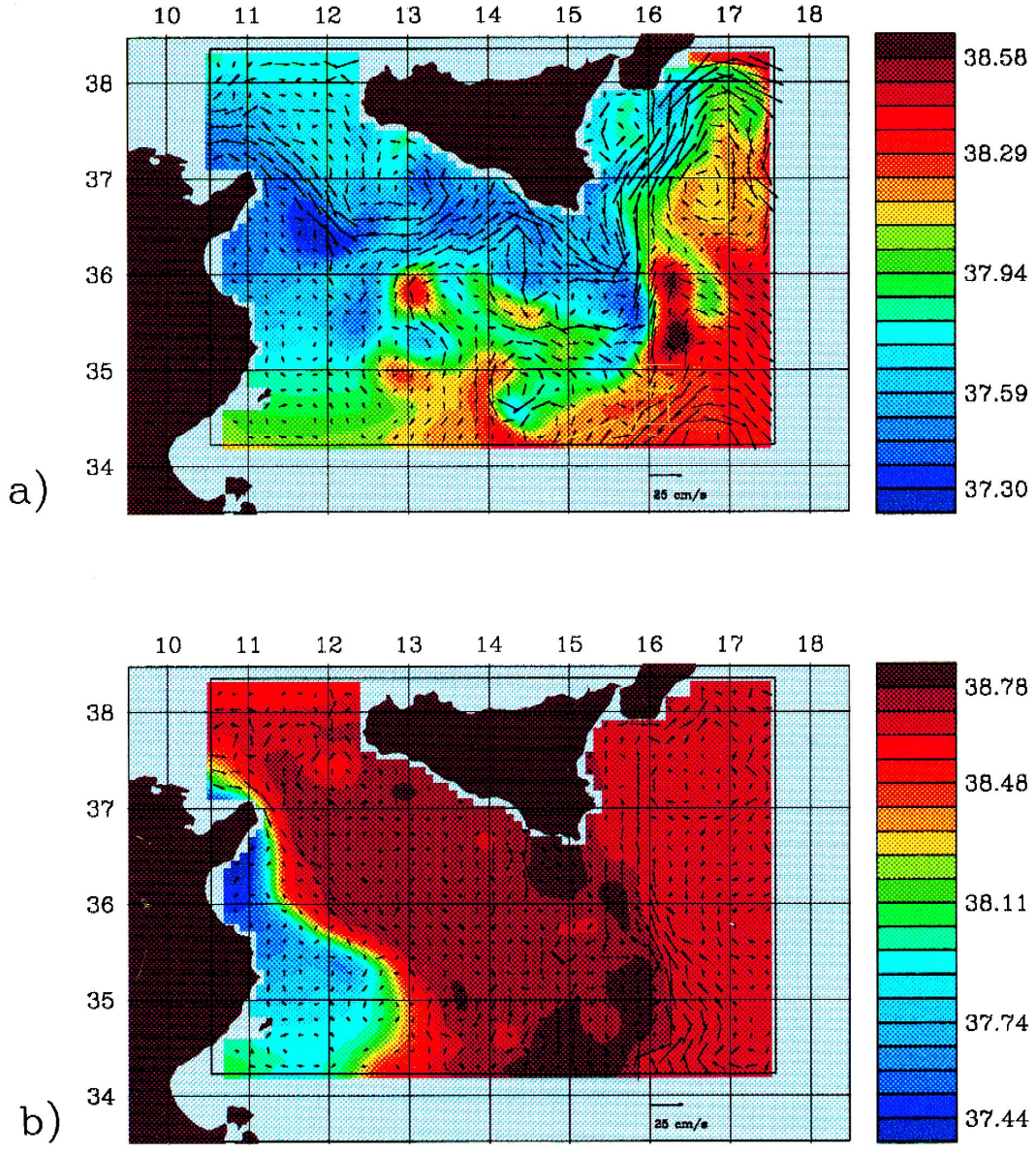

Fig. 9. (a) as above but for salinity. (b) as in (a) but for a model level representing the depth of LIW.

configuration consisted of 83 underwater units, 8 for temperature and pressure, 75 for temperature and conductivity, all molded in sensor fins of postcard size and strung on a 10 mm cable of 240 m length. The cable was held down by a venetian blind type depressor. On its upper end it was mounted below a surface float, which was towed behind the ship. By this means the towed chain was decoupled from the ship's heaving. The sensor fins were inductively coupled to the towing cable. The power for the sensor electronics was drawn off the frequency, which was sent down the cable by the deck unit. Commands from the deck unit to the chain sensors and data messages back to the deck unit were sent as frequency encoded bit-serial binary data. Transmission speed was 9600 Bit/s. The duration of a full

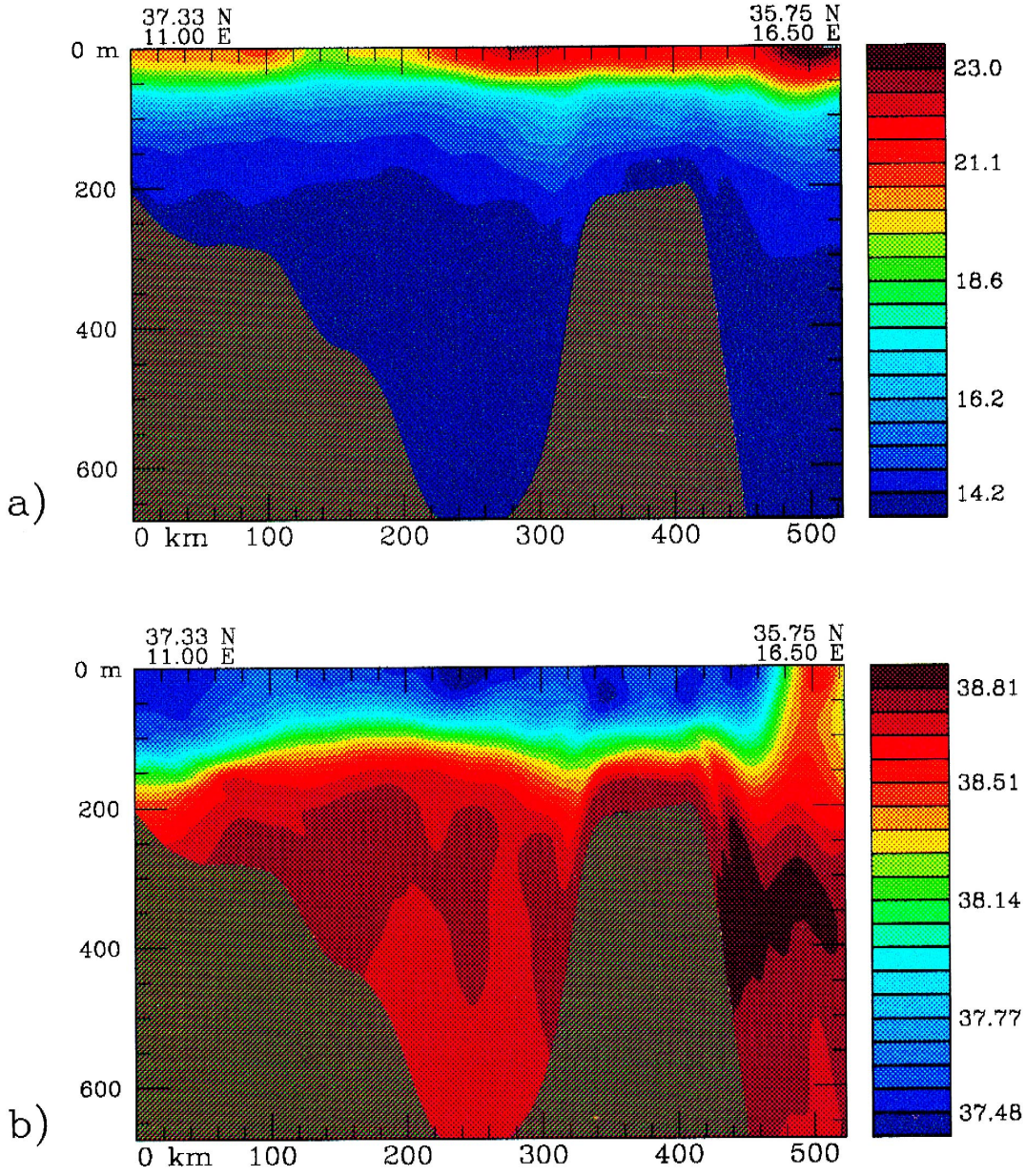

Fig. 10. Vertical section along track O during AIS95 of (a) temperature, and (b) salinity.

chain data cycle was 2 s. Horizontal and vertical resolutions of temperature and salinity were about 5 and 2.5 m.

The CTD chain was towed for two sections across the Sicilian Channel a zig-zag on the shelf break NE of Malta, and a section through the Strait of Messina (Fig. 2b). Generally on scales below 10 km the temperature and salinity profiles were influenced more by mutual intrusions of water masses of different origin than by gravity driven displacement of isolines, the density contours being relatively smooth. Fig. 11 as an interesting example of a section cross-

ing the Atlantic Ionian Stream (AIS) flowing northward along the shelf break. The measurements were horizontally compressed to fit into the figure. Wavelengths below 100 m are therefore not visible in the plot. Temperature, salinity and density are color coded according to the color bars. Note that, for density, the color bar presents the sigma–T values only in the middle of the range of densities presented. For the lower densities (upper ocean) and the higher densities (deeper ocean), 1.5 kg/m^3 must be subtracted or added. The depths of the uppermost and deepest sensors are evident as the upper and lower bounds of the colored area. The tracks of the other sensors became invisible when the gaps were filled by linear vertical interpolation.

The section of Fig. 11 which starts at 36°13′N, 15°23′E (less than three miles from a current meter mooring on 600 m water depth) and ends at 36°24′N, 15°58′E in more than 3000 m depth, is indicated on Fig. 8. The density maximum at the surface close to the western margin (A) of the section is the surface indication of the shelf break front. The connected culmination points of the isopycnals that slope down to the west result in a slope of 1:110 that intersects the shelf edge. East of the front, the Levantine Intermediate Water (LIW, $S > 38.8$) rises to less than 150 m depth.

Calculations and measurements give a consistent picture of the currents in the area of the section: dynamic analysis from CTD profiles shows the center of a cyclonic eddy located at the western end of the section. The current meter measurements from the mooring at this point are highly variable in direction and low in speed. At the time of the towed chain measurements it was 5 cm/s at 20° direction at 17 m depth, 10 cm/s at 335° at 59 m and almost zero in 197 and 570 m depth. For surface drifters that had been deployed for a few days were circling around the mooring position. Finally, the shipboard ADCP measured northward flow with speeds up to 50 cm/s along the tow track.

In the location of the towed chain section, the Modified Atlantic Water formed a stream that turned SE at the Sicilian coast and crossed the Malta Plateau east of Malta (Fig. 8). At the shelf break it made a turn to north. After arrival in the Ionian Sea, the core of this Atlantic Ionian Stream (AIS) had a salinity of less than 37.4 psu and a speed of 25 to 50 cm/s. The warmer and more saline water in the surface layer of the eastern half of the section was slower than the AIS water in the thermocline below. Footprints of small scale dynamics are noticeable in the density section especially at this boundary of the stream. Here the pycnocline displacements were up to 10 m. In the middle part of the section, amplitudes of internal waves in the range from less than 100 to 1000 m were of the order of meters. The zig-zag tow tracks were not all equal in length, but there are two other tracks that also cross the full width of the AIS in the Ionian Sea. The sections of these tracks are very similar.

3.2. Water masses

From the hydrocast survey data obtained during the AIS 94 and AIS95 cruises, we have derived a water mass model. Fig. 12 is a schematic composite of the observed vertical temperature and salinity profiles. The measured shapes of the profiles suggest the presence of seven water masses. From the surface downwards they are: Surface, Upper, Atlantic, Mixed, Fresh, Transition and Levantine. Any individual profile is not likely to be composed of all of the seven water masses; this water mass model depicts those which are possible to occur in an actual profile in this region. The core Atlantic water mass below the surface layer is outlined by a cusp shaped salinity distribution. The Atlantic water is identified by the salinity minimum. It is capped by the upper water layer above and the mixed region below, where the salinity tends to change linearly. On top of the Atlantic core location, an upper layer is sometimes located below the surface region and is distinguished by a relatively high value of salinity, together with a mixed temperature distribution. At the bottom, Levantine water is present with a transition region above. Between the mixed and transition layers, a fresh water region identified by lower salinity values occurred, on occasion, with relatively lower temperatures.

The peak frequency of the occurrence of the depth of the Atlantic water minimum salinity value (Atlantic Extremum [AE]) tends to be around 70 m, suggesting a shallow near surface location for the core of the Atlantic water and the associated current (AIS), Fig. 13. Less frequent occurrences of other

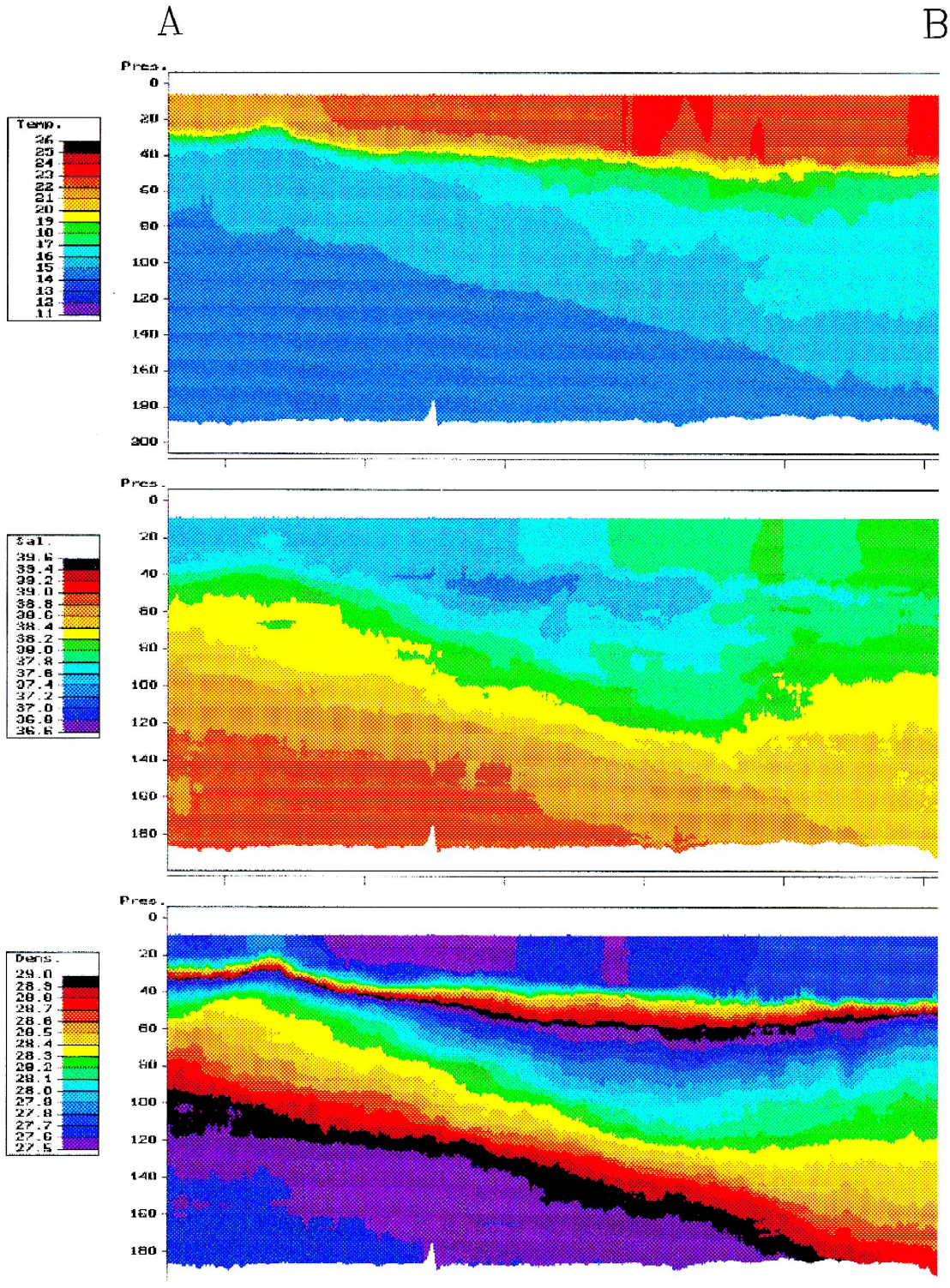
A
B
Pres.
Temp.
Sal.
Dens.

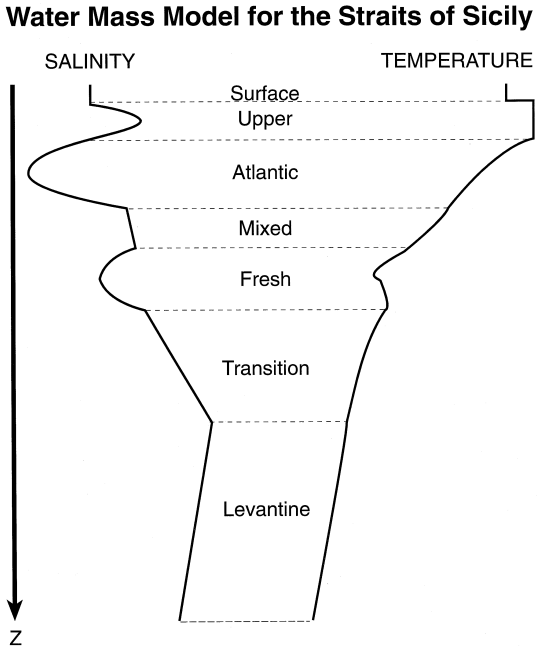

Fig. 12. Schematic water mass model.

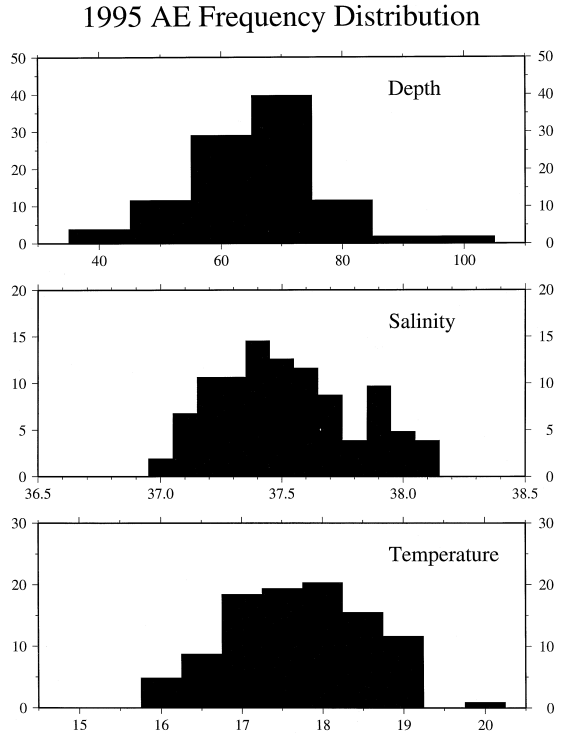

Fig. 13. Frequency distribution of depth, salinity and temperature for the Atlantic Water minimum salinity value-Atlantic Extremum (AE).

depths are present with values of 40 and 100 m, resulting in a 60 m variation. Fig. 13 also indicates the salinity and temperature values associated with the AE. Salinities range from 37.0 to 38.1, with the envelope peaking at around 37.4. Corresponding temperatures range from 16 to 19 degrees and peak around 18.

Previous analysis of POEM data by Moretti et al. (1993) considered the surveys of October 1986, March 1987, August 1988, October 1989, and March 1990. They assumed that the Atlantic water occupies the upper 100 m and showed that the salinity distribution has a nucleus of low salinity formed by the core of Atlantic water. A jet-like meandering of Atlantic water was found from one survey to another. The salinity minimum contour values, deduced from the October 1989 survey, ranged from 37.2 to 37.7. This spread is encompassed in the AE salinity frequency diagram.

The objectively analyzed AE depth distributions, Fig. 14a, depicts the spatial location of the extremum depths. Dots on the figure indicate the observation locations, where high confidence is given to the analysis. The core extremum tends to be shallow along the Sicilian coast and shelfbreak. The calculated thicknesses of the Atlantic layer core yield values around 35 m along the coast, increasing to 60 further away.

Objective analyses of the temperature and salinity at the core of the Atlantic Water are shown in Fig. 14b and c. These plots show colder temperature and lower salinities along the Sicilian coast and onto the shelfbreak. Temperatures and salinities are higher away from the coast and east of the shelfbreak in the Ionian Sea.

Fig. 11. Vertical sections of temperature, salinity and density across the shelf break from the Malta Plateau to the Ionian Sea measured with a towed CTD chain during AIS95 along the path indicated in Fig. 8. Tick marks every 9.6 km denote full hours of towing.

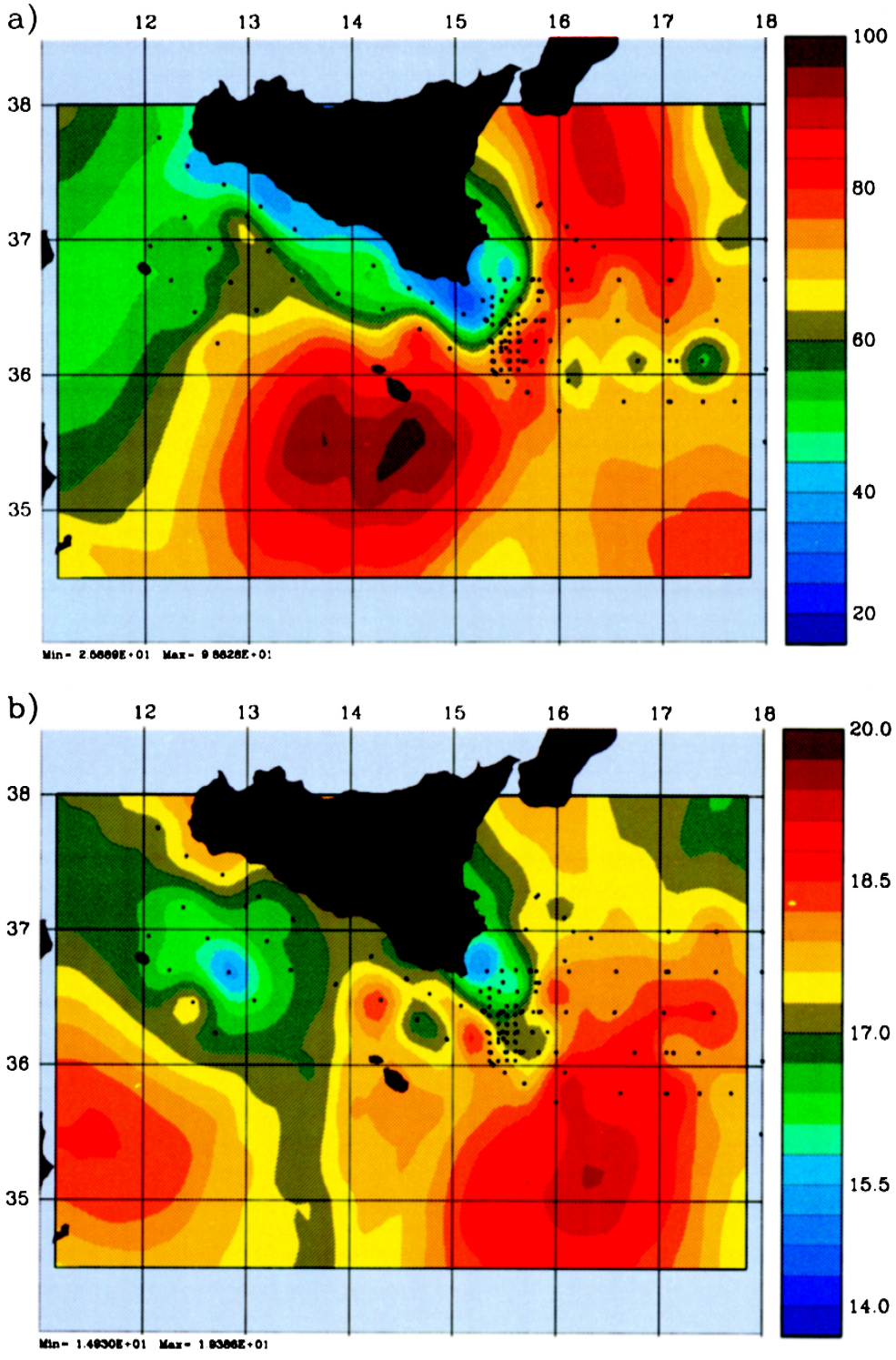

Fig. 14. Objective analyses of AE layer parameters; (a) depth, (b) temperature, (c) salinity.

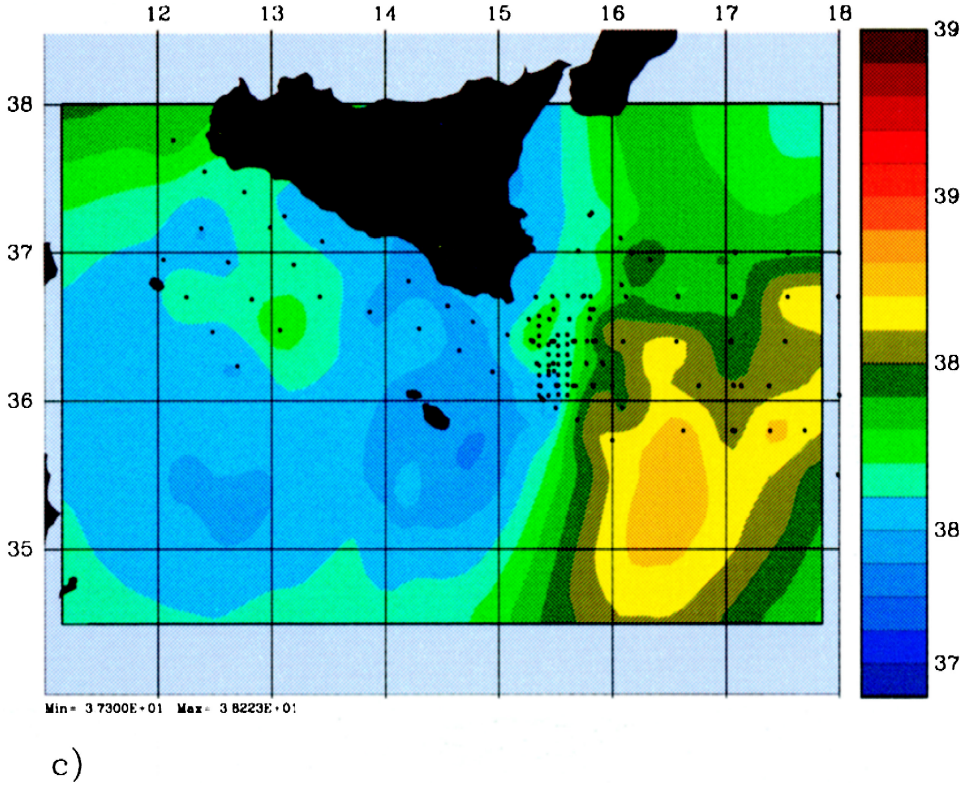

Fig. 14 (continued).

The *TS* relationship for the AIS95 data is shown in Fig. 15. Fig. 15a indicates the values for all depths. Fig. 15b includes data deeper than 50 m and Fig. 15c includes only data deeper than 100 m. The shallow data is warm with a wide range of salinities. It is located in the mixed layer region, whose depth range was from 40 m to 50 m. There are isothermal layers which have variations in salinity of up to 0.8. Data between 50 m and 100 m represent Modified Atlantic Water, with salinities ranging from approximately 37.2 to 38.3, and temperatures ranging from 16.6 to 19°C. The most frequently occurring temperatures and salinities associated with the center location of the Atlantic Water core (Fig. 13), fall in the same value range. The deeper temperature and salinity values indicate two water masses: Levantine Intermediate Water (LIW) and Adriatic (or Eastern Mediterranean) Deep Water (ADW). The LIW is indicated by the salinity maximum of the *TS* relationship. The ADW (or EMDW) is indicated by the colder, fresher water at the bottom of the casts.

4. Variability and prediction

4.1. Nowcasting / forecasting

The development of a regional forecast system for the Strait of Sicily has been ongoing since November 1994. Dedicated data from cruises in that month (AIS94) and in October 1995 (AIS95) have been utilized within the Harvard Ocean Prediction System (HOPS) in the exploratory and dynamical stages of the forecast system development (Lozano et al., 1996; Robinson et al., 1996). In August 1996 (AIS96) HOPS was utilized during the NATO Rapid Response exercise (Sellschopp and Robinson, 1997; Robinson, 1997) for rapidly determining the synoptic state of the ocean (and the relevant parameters for

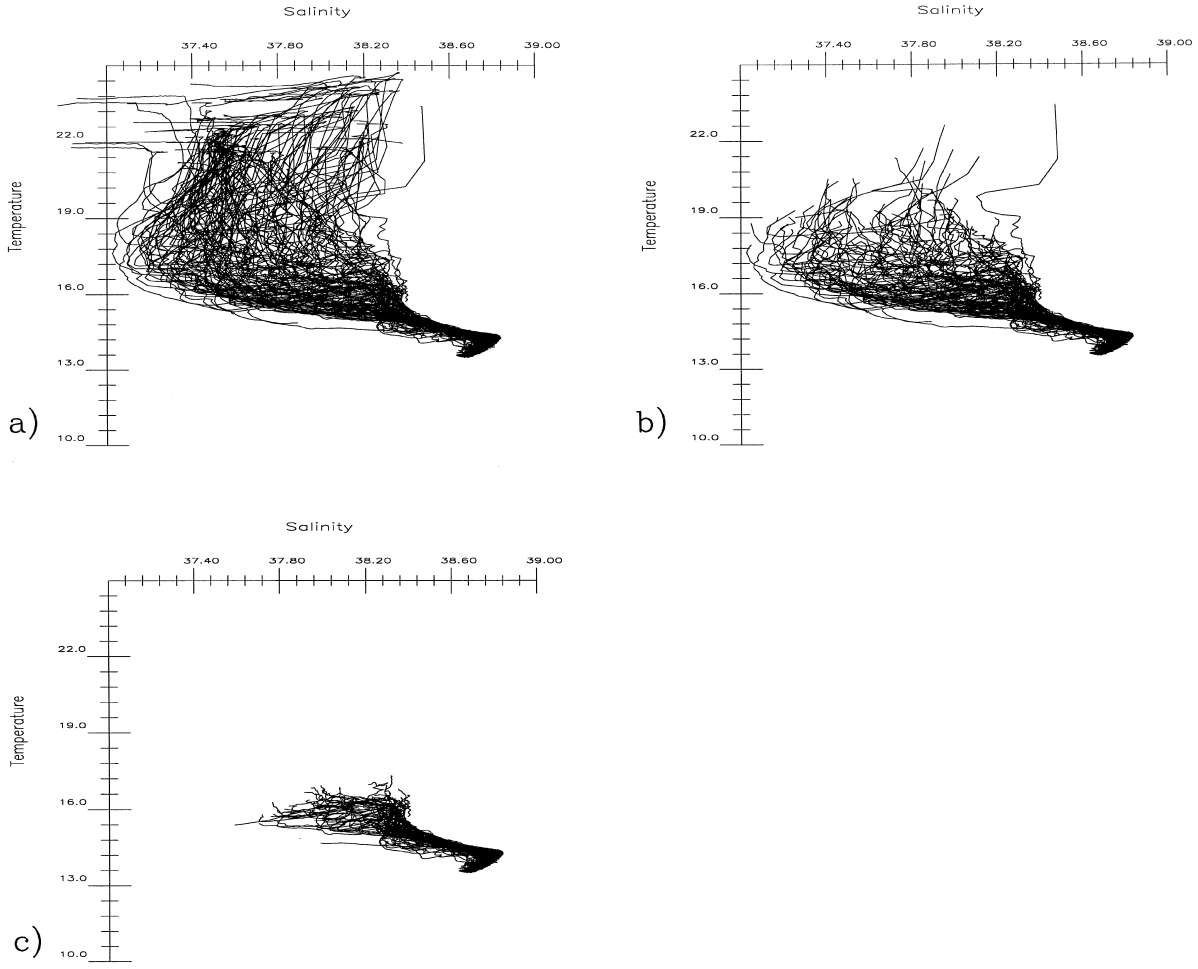

Fig. 15. T/S plots of AIS95 hydrographic data; (a) all depths, (b) depths below 50 m, (c) depths below 100 m.

naval operations) and forecasting in real-time the evolution of the local conditions for naval exercises.

The configuration of HOPS for the AIS96 exercise included: (i) data sets for the region (MODB2 climatology, AIS94-AIS95 synoptic data sets, statistical parameters); (ii) data quality control modules; (iii) procedures to grid the observations (objective analyses, melding, vertical extensions); (iv) procedures to prepare initialization fields for the dynamical model (utilization of CTD/XCTD salinity data with AXBT and XBT casts; velocity field estimation); (v) data assimilation procedures to meld dynamical model output and data (optimal interpolation); (vi) procedures to prepare estimates of atmospheric fluxes (wind stress, heat and water fluxes) using FNOC fields; (vii) primitive equation model (PE) to evolve in time temperature, salinity and velocity fields; and, (viii) procedures to prepare graphical displays and data exports. The near surface portion of HOPS has high resolution physics appropriate to the surface boundary layer. The necessary fields of wind stress, heat fluxes, short and long wave radiation fluxes, and evaporation rates have been derived from FNOC analyses and forecasts. The analyses, simulations, hindcasts and forecasts were used to define current synoptic conditions,

describe a 'typical' synoptic picture, depict possible future states or illustrate the potential extremes of variability.

The real-time experiment in 1996 had two phases. In the first, data was gathered and utilized by HOPS at sea aboard the NRV Alliance. Data was available both from shipboard hydrographic observations and from AXBT data relayed to the ship. Data gathering schemes evolved underway, a form of 'adaptive sampling', as nowcasts and forecasts helped to determine regions in which data collection was most necessary. During the second phase of operations, HOPS was set up at the SACLANT Centre in La Spezia, Italy. Data was supplied on an ongoing basis by ships participating in the NATO Rapid Response exercise and by a series of AXBT flights. The tracks

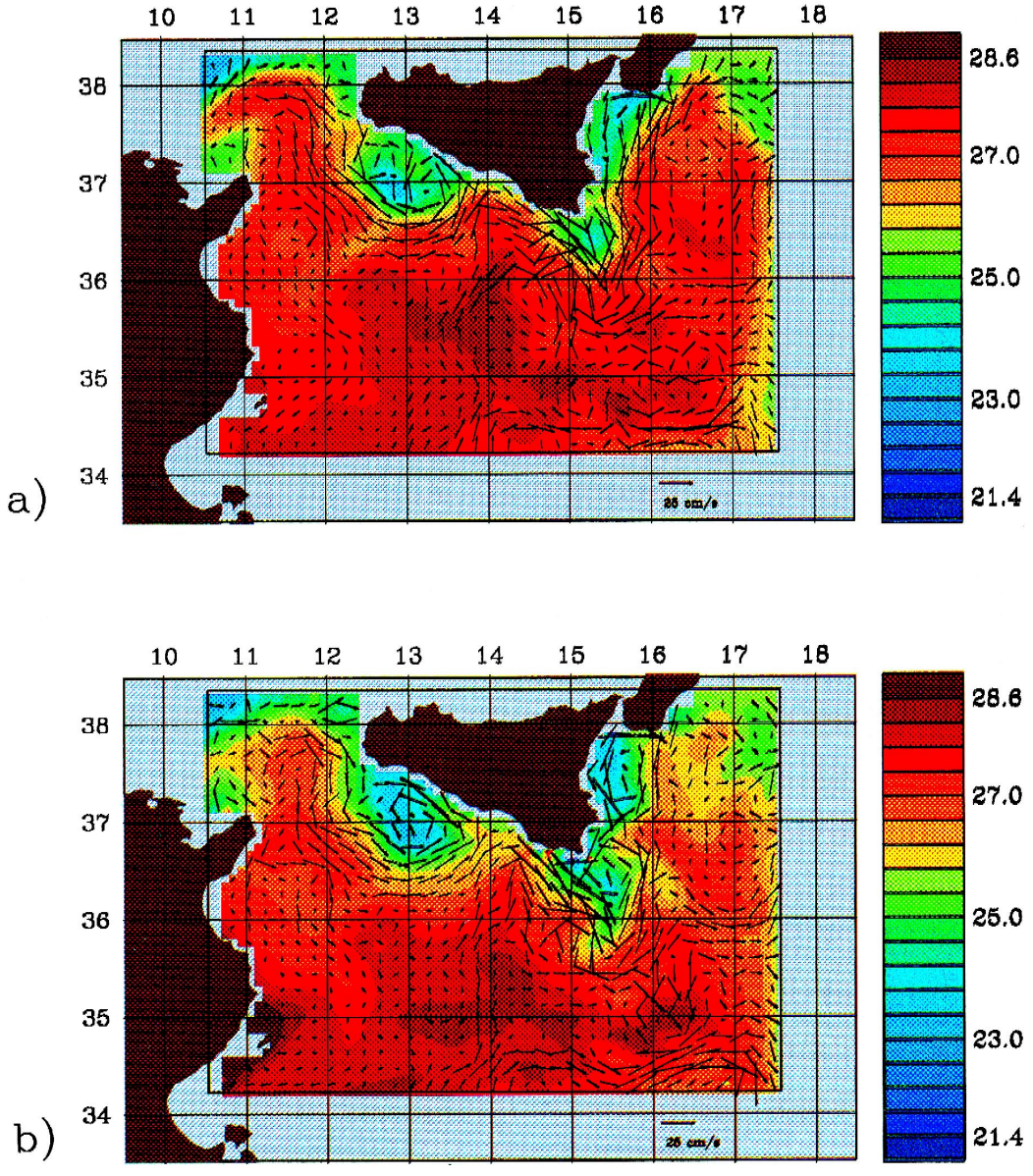

Fig. 16. (a) Dynamical analysis of surface temperature for 22 August 1996. (b) Dynamical forecast of surface temperature for 25 August 1996.

of the AXBT flights were designed to maximize data gathering resources and to acquire information on the most rapidly evolving conditions. Here we give an overview of the hindcasts and predictions which took place and an evaluation of the predictive capability of the system.

From 12–24 August 1996, the NRV Alliance performed 168 CTD, XCTD and XCTD stations; five AXBT flights gathered an additional 225 temperature profiles. This nearly-synoptic data was used in conjunction with dynamically modified historical synoptic data to provide underway at-sea forecasts. The use of historical synoptic data allows for immediate model initialization with synoptic features in place while data gathering proceeds to define the present feature locations. As additional data is gathered and assimilated, the reliance on historical data and climatology is reduced. At the start of the exercise, a first guess synoptic realization was prepared by warming the October 1995 realization to August conditions by artificial surface heating of the fields while under the constraint of primitive equation dynamics. As it was acquired by the ship, hydrographic data was assimilated into this circulation and by 24 August only contemporary data was utilized in the forecast methodology.

Fig. 16a illustrates the dynamical analysis (nowcast) of surface temperature for 22 August. Conditions are generally warm, with the Atlantic Ionian Stream (AIS) defining the boundary between cooler coastal waters and warmer off-shore waters. Major features consistently apparent in this region are: the inflow position of the AIS (Western Sill Jet), the Adventure Bank Vortex (ABV), the crest of the AIS in the Malta Channel (MCC), the Ionian Shelf Break Vortex (IBV) and the East Sicilian Vortex. Significant variabilities which are noted of the major features of the region include: the size, position and shape of the vortices, the relative strength of the AIS, the location of the AIS and the tendencies of the motions.

The ABV is essentially completely enclosed by the surrounding warmer waters. Surface temperatures in the core of the vortex are approximately 24°C. The center of the vortex is located at roughly 37.1°N, 12.8°E. The Sicily Strait sill is warm up to the coastline. Surface temperatures on the sill are in the 25.5–27°C range.

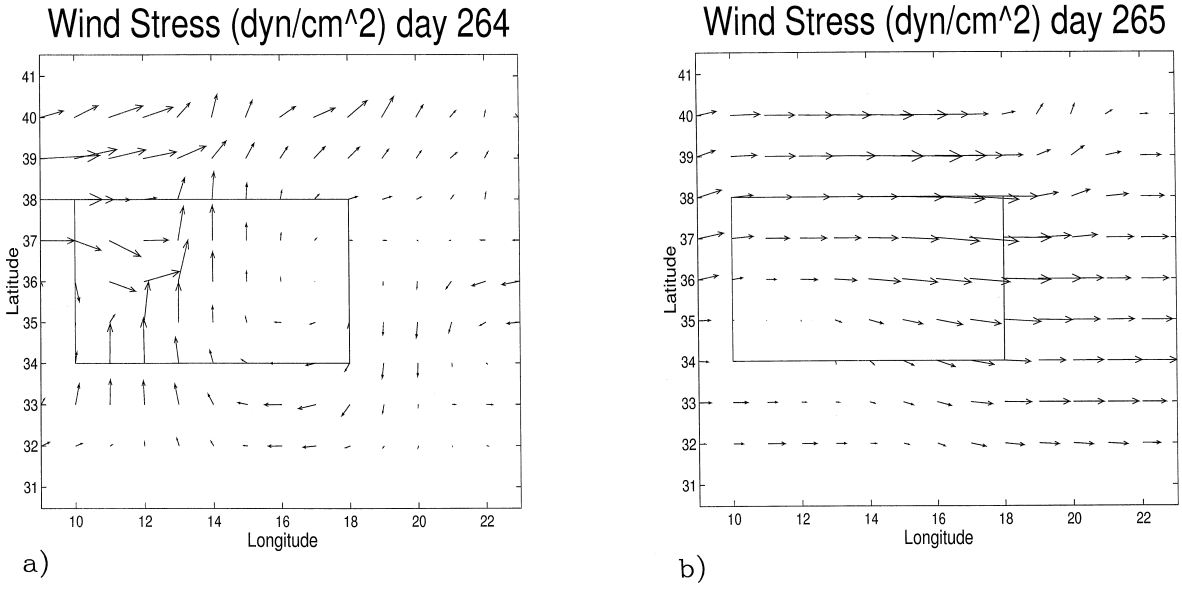

Fig. 17. Surface wind stress fields; (a) 20 September 1996, (b) 21 September 1996.

The MCC of the AIS is located close to the coast of Sicily, with its closest proximity at 14.5°E. The IBV is small, centered at 36.4°N, 15.3°E.

A forecast to 25 August from 22 August was performed onboard ship during the AIS-96 cruise. The results, Fig. 16b, show the changes in the mesoscale field structure and the features of reference. The ABV has become more elongated with a change of AIS structure around its perimeter and has extended eastward to about 14°E. The MCC has been displaced southeastwards. The IBV has enlarged and penetrated further south, causing a change in the AIS structure there. For a visual comparison of the model forecast with satellite observations, compare Fig. 16b with Fig. 1. The verification of model results with IR is quite good for this time period.

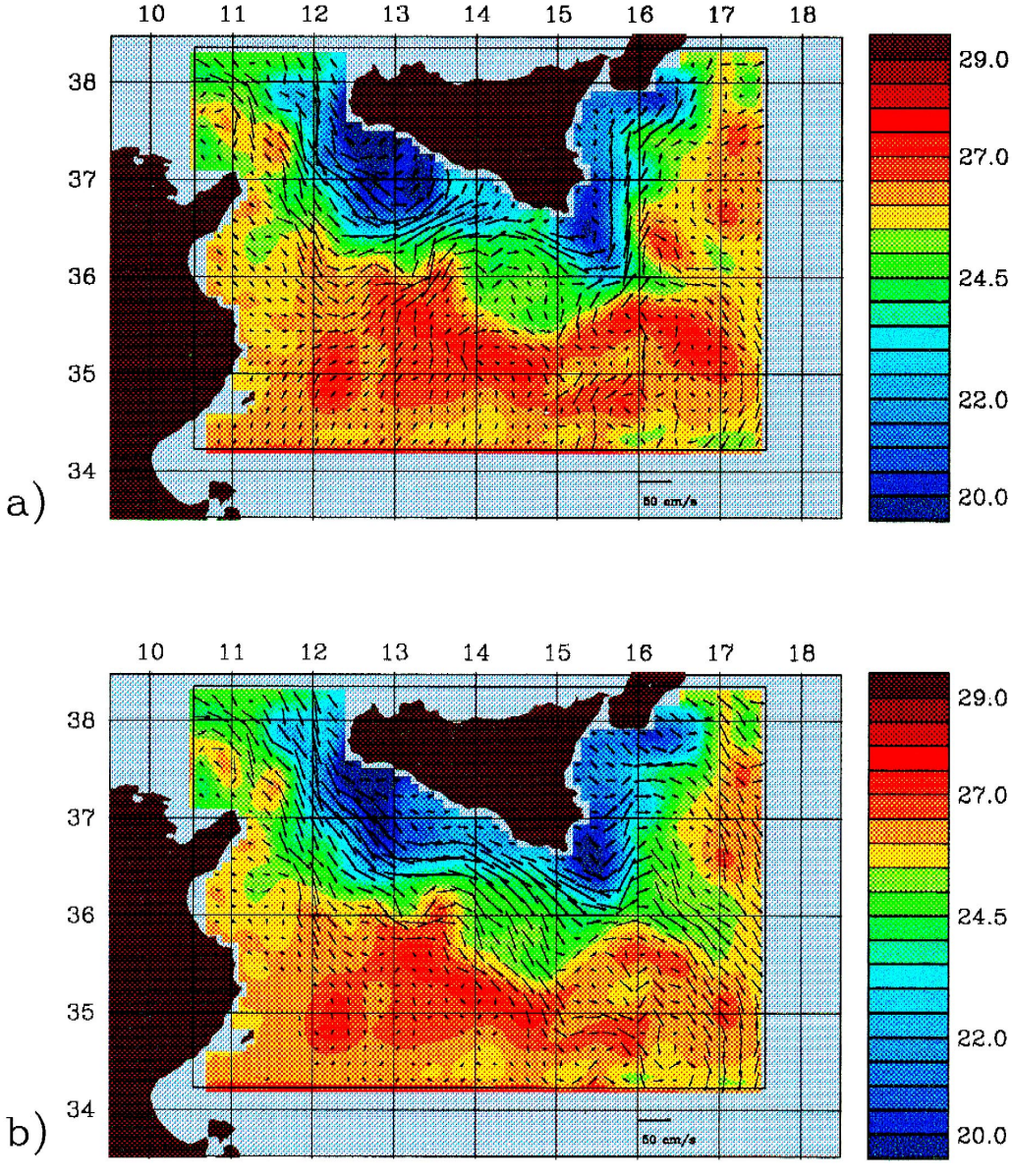

Fig. 18. (a) Forecast surface temperature for 20 September. (b) Forecast surface temperature for 21 September.

Over the period 24 August–15 September, the time of the NATO exercise Rapid Response, 520 additional profiles were added to the data set. This data was assimilated into the forecast system on an ongoing basis, leading to the issuance of dynamical nowcasts and forecasts on 28 and 31 August and 4 September. These nowcasts and forecasts were made immediately available to the NATO community via the exercise web page.

All data gathered prior to 9 September has been used to create the dynamical analysis (nowcast) for 15 September (Fig. 19a). This data set, is that data set used during the continuing Rapid Response forecasting period, augmented by an AXBT flight on 15 September. The general conditions have cooled in response to the changing seasons and the major features have changed in size and shape, when compared to 22 August.

The ABV is expanded in size as compared to 22 August and is no longer completely enclosed by surrounding warmer waters. Surface temperatures have decreased to 21–22°C. The vortex is elongated in the NW–SE direction. At the coastline, the Sicily Strait sill temperatures are 5–6°C cooler than in August.

The crest of the AIS in the Malta Channel has flattened and moved southwards; with the AIS having more E–W orientation. The crest reaches its maximum at about 36.5°N, 14°E. The IBV is large, now reaching as far south as 36°N. The AIS has moved offshore, with its northward flowing branch located at 16°E.

The local forcing was derived from FNOC forecasted fields and is shown in Fig. 17. The forcing pattern distribution are taken to be constant for the day. The wind stress pattern changes from a dominant north–south orientation on 20 September (Julian day 264) to a east–west distribution on 21 September (Julian day 265). Four and five day forecasts for the 20th and 21st of September are shown in Fig. 18. These forecasts were forced by internal dynamical processes and direct response to the local atmospheric forcing. We note the effect of the wind stress orientation on the surface flow (level 1) and the features that we have been following. The 20 September wind stress tends to drive the flow on shore. The 21 September distribution tends to push the flow to the right of the wind and away from the coast.

On 20 September, the ABV has moved onshore and has been further elongated in the NW–SE direction. The inflow of the AIS has a more onshore component than on 16 September. Surface temperatures are largely unchanged over the 1-week period.

On 20 September the crest of the AIS in the Malta Channel is moving back towards the Sicilian coast, there the AIS has regained some of its 'arch' shape. The crest's maximum is now located at 36.6°N,

Table 3

	Adventure Bank Vortex	Malta Channel Crest	Ionian Shelf Break Vortex
(1) Satellite surface temperature			
23 August	Medium size W of 14 E	Close to Sicily about 14.5 E	Small N of 36 N
25 August	Extends E to 14 E	Moves to SE	Enlarges extends S
27 August	A little more to S	Similar to 23 Aug moves N	Smaller or same
07 September	A little more to S Indented meander	Moves to SE as 25 Aug	Extends E to 16 E
(2) HOPS nowcast (dynamic analysis of available data)			
22 August	Medium size W of 14 E	High centered on 14 E	Small N of 36 N W of 15.75 E
28 August	Square, moves E across 14 E	14.5 E Moves to SE	Enlarges, moves S, extends E
31 August	Still straight on the W, moves N on the E	N at 14 E	Similar to 28
04 September	Similar to 22 Aug	N at 14 E	Moves slightly NW
(3) HOPS forecast for 2 or 3 days			
25 August	As nowcast (++)	As nowcast (++)	As nowcast (++)
30 August	Square but wrong orientation	Remains SE of 14 E (−)	Similar (+)
03 September	Retains shape (++)	N at 14 E (++)	Slightly E (−)
07 September	W edge moves W (++)	Perhaps slight SE (++)	Extends to S (+)

14.25°E. The IBV is reduced slightly in size, now only reaching as far south as 36.25°N. The northward flowing branch of the AIS is essentially unchanged in the shelfbreak region.

4.2. Verification

A quick-look verification of predicted variations in the Sicilian Channel was performed for four cases of the Rapid Response survey as Rapid Response proceeded. The satellite sea surface temperature images of 23 (1736Z), 25 (1259Z), and 27 (1237Z) August and 7 (1218Z) September and the HOPS nowcasts of 22, 28 and 31 August and 4 September have been selected and the position and shape of three dominant features are described, as well as their development in time. The satellite images were

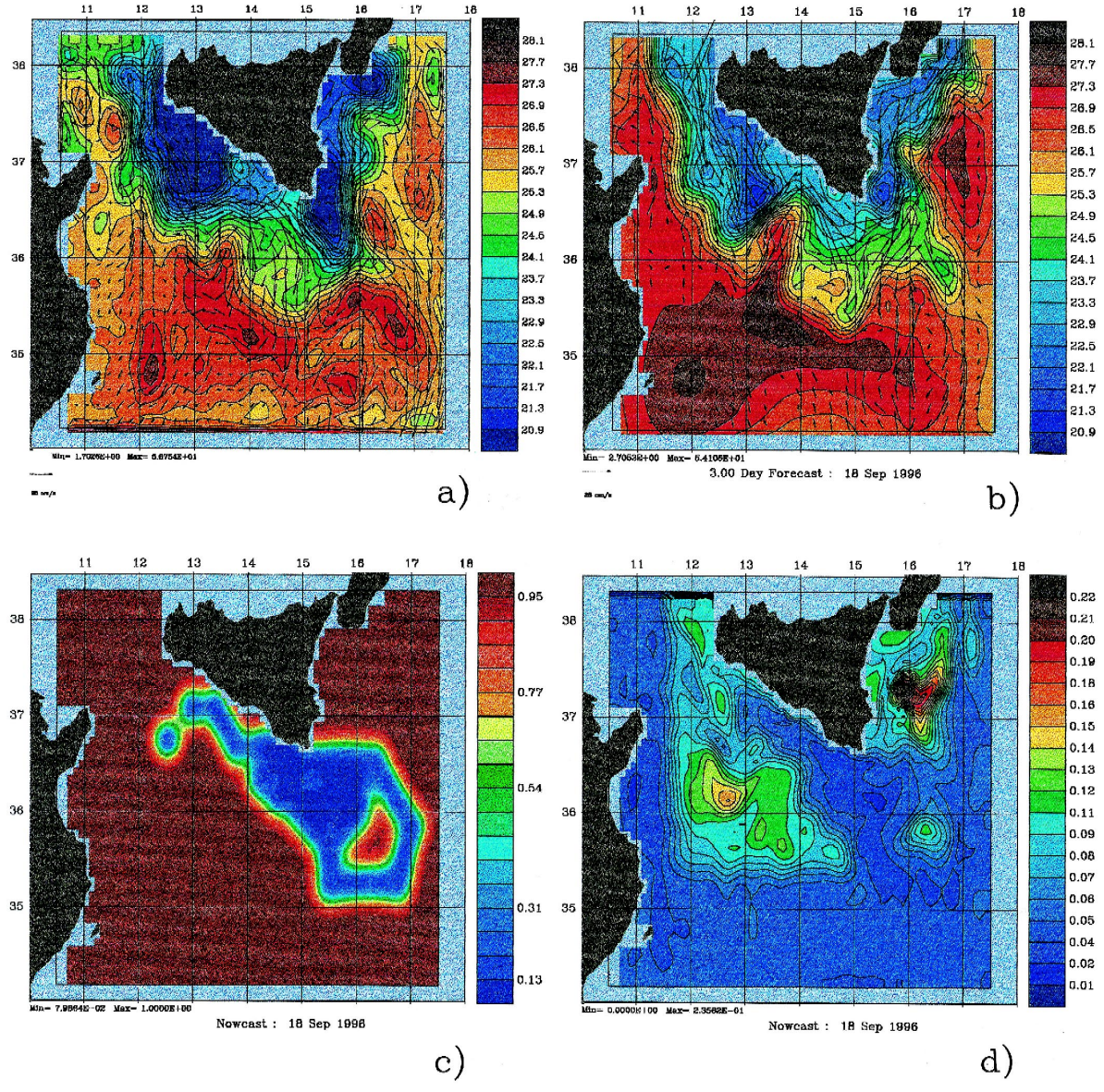

Fig. 19. (a) Dynamical analysis of surface temperature for 15 September 1996. (b) ESSE forecast for 18 September. (c) Error field from objective analysis. (d) Error field from ESSE forecast.

chosen with regard to percentage cloud cover. The quick-look comparison of actual development versus predicted development for 25 and 30 August and 3 and 7 September indicates that the HOPS forecasts successfully predicted conditions at a success rate of approximately 70%. Table 3 presents the subjective analyses of three of the major local features as depicted by the: SST data, HOPS nowcast and HOPS forecast. Nine of the 12 comparisons agreed very well (++) or well (+).

4.3. ESSE forecast

The AIS96 experiment provided an opportunity to implement, in real-time, a newly developed data assimilation methodology. This methodology is based on an optimal reduction of the dimension of error covariance and has led to the notion of an evolving Error Subspace (ES), characterized by singular error vectors and values, or, in other words, the error EOFs. This defines the concept of Error Subspace Statistical Estimation (ESSE) (see the Appendix A). The ideal Error Subspace spans and tracks the scales and processes where the dominant, most energetic, errors occur. The methodology is, therefore, especially well suited for the concept of adaptive sampling; identifying dominant errors and modifying sampling patterns to investigate those regions. Fig. 19b–d illustrates the results and products of a 3-day ESSE forecast. Fig. 19b shows the results of a 3-day ESSE forecast from the conditions on 15 September. Fig. 19c and d depict the error fields from the objective analysis of data to be assimilated and the ESSE forecast errors, respectively. The data being assimilated reduces the error field in the forecast. The 'hot spots' of error in the forecast error field indicate regions which, in the sense of operational sampling, are in need of investigation.

5. Summary and conclusions

The SACLANT Undersea Research Centre and Harvard University have been developing a regional descriptive and predictive capability for the Strait of Sicily. The aims of the work have been to: (1) design of an regional forecasting system; (2) rapid assessment of regional phenomena, scales, processes, and interactions; (3) determination, with assimilated real time data into the Harvard Ocean Prediction System, of synoptical flow structures and dynamical events; (4) identification of the water masses in the Strait of Sicily; and, (5) studies of the AIS structure and variability. The development of a predictive capability for the Strait of Sicily region has evolved through three phases. Those three phases are: exploratory, dynamical, and predictive.

Dedicated cruises have taken place in 1994, 1995 and 1996. During each cruise, data was assimilated in real-time, at sea, as it became available. Adaptive sampling, based on shipboard predictions, was used to investigate potentially interesting phenomena. Forecast experiments have been performed with these high quality data sets and have described the regional circulation, dynamics, variabilities, exchanges, and interactions.

From the hydrography data obtained during the AIS-95 and AIS-95 surveys, we have derived a water mass model. The measured temperature and salinity distributions suggested seven water masses. From the surface downwards these were: Surface, Upper, Atlantic, Mixed, Fresh, Transition, and Levantine water masses.

A picture of some semi-permanent features which occur in the Strait of Sicily, as part of the AIS circulation structure, is beginning to emerge. Dynamical circulation studies, with assimilated data from surveys, indicate the presence of an Adventure Bank Vortex (ABV), Maltese Channel Crest (MCC), and Ionian Shelf Break Vortex (IBV).

A quick verification of the predicted AIS variations in the Strait of Sicily was performed for four cases. These involved satellite sea surface images on 23, 25, and 27 August and 7 September. The quick-look comparison of actual development versus predicted developments for 25 and 30 August and 3 and 7 September show that the HOPS predicted conditions were correct approximately 70% of the time.

Acknowledgements

The observations discussed in this work were obtained via the skilled data acquisition and processing abilities of the CTD/XCTD/XBT support staff of SACLANTCEN's Applied Oceanography Group, Ocean Engineering Department and Digital Computer Department and the captain and crew of the

Table 4
Minimum sample ES variance linear update (index k omitted)

Dynamical state update	$\hat{\boldsymbol{\psi}}(+) = \hat{\boldsymbol{\psi}}(-) + \mathbf{K}^s[\mathrm{d} - \mathbf{C}\hat{\boldsymbol{\psi}}(-)]$	(A1)
Sample ES optimal gain	$\mathbf{K}^s = \mathbf{E}^s_- \boldsymbol{\Pi}^s(-)\tilde{\mathbf{C}}^{\mathrm{T}}[\tilde{\mathbf{C}}\boldsymbol{\Pi}^s(-)\tilde{\mathbf{C}}^{\mathrm{T}} + \mathbf{R}]^{-1} = \mathbf{E}^s_- \tilde{\mathbf{K}}^s$ with $\tilde{\mathbf{C}} = \mathbf{C}\mathbf{E}^s_-$, $\mathbf{M}(-) \simeq \mathbf{E}^s_- \boldsymbol{\Sigma}^s(-)\mathbf{V}^{s}_-$, and $\boldsymbol{\Pi}^s(-) = (\boldsymbol{\Sigma}^{s2}(-)/q)$,	(A2)
Sample ES update	$\mathbf{H}^s\boldsymbol{\Pi}^s(+)\mathbf{H}^{s\mathrm{T}} = \tilde{\boldsymbol{\Pi}}^s(+) = (\boldsymbol{I}_p - \tilde{\mathbf{K}}^s)\boldsymbol{\Pi}^s(-)$	(A3)
	$\mathbf{E}^s_+ = \mathbf{E}^s_- \mathbf{H}^s$	(A4)

NRV Alliance. Marsha Glass supplied invaluable logistical assistance. The Fleet Numerical Oceanographic Center (FNOC) provided the NODDS products. This research was supported at Harvard University by the Office of Naval Research under contracts N00014-90-J-1612 and N00014-95-1-0371 and by the National Science Foundation under contract OCE-9403467.

Appendix A. Data assimilation via error subspace statistical estimation

This appendix presents a brief description of the filtering part of an Error Subspace Statistical Estimation (ESSE) hybrid method solving a 'nonlinear smoothing statistical estimation problem'. For a more complete presentation, with nonlinear smoothing schemes via ESSE, refer to Lermusiaux (1997).

A rational approach has been used to identify an efficient statistical estimation scheme for data assimilation in nonlinear ocean/atmosphere models. The conditional mean estimate, a minimum of several cost functionals, is chosen for an optimal estimate. General observed characteristics of ocean measurements and models are utilized to approximate this estimate. The sub-optimal criterion is based on a continued and energetically optimal reduction of the dimension of error covariances. This leads to the notion of an evolving Error Subspace (ES), of variable size, characterized by error singular vectors and values, or in other words, the error EOF's and coefficients.

An algorithm is described here after for filtering via ESSE. Table 4 describes the minimum error variance melding within the Error Subspace, which is much less costly than classical analyses involving full error covariances. The Error Subspace covariance is updated at the melding step by combining its forecast, which is the sum of the principal dynamical model and loss of predictability errors, with the measurement model error covariance. The estimate of the dynamical state vector at time t_k is denoted by

Table 5
Nonlinear dynamical state and ES ensemble forecast

Central Dynamical		
State forecast	$\hat{\boldsymbol{\psi}}_{k+1}(-) = f_k\big(\hat{\boldsymbol{\psi}}_k(+)\big)$. Note: chosen forecast can be ensemble mean, central forecast or most probable forecast.	(A5)
ES initial conditions	$\hat{\boldsymbol{\psi}}^j_k(+) = \hat{\boldsymbol{\psi}}_k(+) + \mathbf{E}_k(+)\boldsymbol{\pi}^j_k(+), \quad j = 1,\ldots,q,$	(A6)
	with either, $\boldsymbol{\pi}^j_k(+) = \boldsymbol{\Pi}^{(1/2)}_k(+)\boldsymbol{u}^j,$	(A7a)
	$\boldsymbol{\pi}^j_k(+) = \boldsymbol{\Pi}^{(1/2)}_k(+)\boldsymbol{u}^j$, with dynamical/data constraints, or,	(A7b)
	$\boldsymbol{\pi}^j_k(+) = \sqrt{q}\,\boldsymbol{\Pi}^{(1/2)}_k(+)\mathbf{H}^{\mathrm{T}}_k(\mathbf{V}_k(-)^{\mathrm{T}})_j$, where $\boldsymbol{u} \sim (0,\ \boldsymbol{I}_p)$.	(A8)
Ensemble forecast	$\hat{\boldsymbol{\psi}}^j_{k+1}(-) = f_k\big(\hat{\boldsymbol{\psi}}^j_k(+)\big) + \hat{\boldsymbol{w}}^j_k, \quad j = 1,\ldots,q,$	(A9)
	where $\hat{\boldsymbol{w}}^j_k = \boldsymbol{B}_k\boldsymbol{u}^j$, $\boldsymbol{Q}_k = \boldsymbol{B}_k\boldsymbol{B}^{\mathrm{T}}_k$ and $\boldsymbol{u} \sim (0, \boldsymbol{I}_r)$.	
ES forecast	$\mathbf{M}^s_{k+1}(-) = \big[\,\hat{\boldsymbol{\psi}}^j_{k+1}(-) - \hat{\boldsymbol{\psi}}_{k+1}(-)\big], \quad j = 1,\ldots,q,$	
	decomposed into, $\boldsymbol{\Pi}_{k+1}(-) = [\,\boldsymbol{\Sigma}^2_{k+1}(-)/q$ and $\mathbf{E}_{k+1}(-)$ of rank $p \le q$, defined by,	
	$\{\boldsymbol{\Sigma}_{k+1}(-), \mathbf{E}_{k+1}(-) \mid \mathrm{SVD}_p(\mathbf{M}^s_{k+1}(-)) = \mathbf{E}_{k+1}(-)\,\boldsymbol{\Sigma}_{k+1}(-)\mathbf{V}^{\mathrm{T}}_{k+1}(-)\}$, where the operator $\mathrm{SVD}_p(\cdot)$ selects the top rank p SVD.	(A10)

$\hat{\boldsymbol{\psi}}_k \in \mathbb{R}^n$, $k = 0, \ldots, N$. All data available at time t_k are contained in the vector $\boldsymbol{d}_k \in \mathbb{R}^m$ and R is the measurement error covariance. $\mathbf{C}^k$ is the measurement model matrix at time t_k, the columns of $\mathbf{E}^s_- \in \mathbb{R}^{n \times p}$ contain the eigenvectors of the error subspace forecast, the diagonal $\boldsymbol{\Pi}^s(-)$ contains the error subspace eigenvalues. The error subspace of size p_k is defined by restricting the sample error covariances to their dominant singular value decomposition. The columns of $\mathbf{M}(-) \in \mathbb{R}^{n \times q}$ constitute an ensemble of (Monte-Carlo) sample error forecast.

Table 5 gives the nonlinear dynamical state and Error Subspace forecast. It is based on an (Monte-Carlo) ensemble forecast which uses the full nonlinear model. To generate the dominant error modes, the members of the ensemble are chosen to optimally sample the current dominant errors. The superscript s has been omitted on $\mathbf{E}_k$, $\mathbf{E}_{k+1}$ and $\boldsymbol{\Pi}_k$, $\boldsymbol{\Pi}_{k+1}$. The vector $\hat{\boldsymbol{w}}^j_k = \boldsymbol{B}_k \boldsymbol{u}^j$ represents is a model error sample, with $\boldsymbol{u} \in \mathbb{R}^r$, $\boldsymbol{u} \sim (0, \boldsymbol{I}_r)$, $_q \geq {}_r$. The matrix $\mathbf{Q}_k = \boldsymbol{B}_k \boldsymbol{B}_k^{\mathrm{T}}$ is the a priori model error covariance over Δt_k. Note that a normalization in multivariate ES is performed, an Error Subspace divergence/convergence criterion is utilized and several Error Subspace forecast variations and specifications exist.

References

Grancini, G.F., Michelato, A., 1987. Current structure and variability in the strait of Sicily and adjacent area. Annales Geophysicae 5b (1), 75–88.

Johannessen, O.A., Good, D., Smallenburger, C., 1977. Observation of an oceanic front in the Ionian Sea during early winter 1970. J. Geophys. Res. 82, 1381–1391.

Lermusiaux, P.F.J., 1997. Error subspace data assimilation methods for ocean field estimation: theory, validation, applications, PhD Thesis, Harvard University, Cambridge, MA.

Lozano, C.J., Robinson, A.R., Arango, H.G., Gangopadhyay, A., Sloan, N.Q., Haley, P.J., Leslie, W.G., 1996. An interdisciplinary ocean prediction system: assimilation strategies and structured data models. In: Malanotte-Rizzoli, P. (Ed.), Modern Approaches to Data Assimilation in Ocean Modelling. Elsevier Oceanography Series, Elsevier Science, The Netherlands. pp. 413–452.

Malanotte-Rizzoli, P., Manca, B., Ribera, M., Theocharis, A., Bergamasco, A., Bregant, D., Budillon, G., Civitarese, G., Georgopoulos, D., Korres, G., Michelato, A., Sansone, E., Scarazzato P., Souvermezoglou, E., 1997. A synthesis of the Ionian Sea hydrography, circulation and water mass pathways during POEM phase I. Prog. Oceanog., submitted.

Manzella, G.M.R., Hopkins, T.S., Minnet, P.J., Nacini, E., 1990. Atlantic water in the strait of Sicily. J.C.R. 95 (C 2).

Moretti, M., Sansone, E., Spezie, G., De Maio, A., 1993. Results of investigations in the Sicily channel, 1986–1990. Deep Sea Research II 40 (6), 1181–1192.

Robinson, A.R., 1997. Forecasting and simulation coastal ocean processes and variabilities with the Harvard ocean prediction system. Proc. Int. Conf. Rapid Environmental Assessment, Lerici, Italy, Mar. 10–14, 1997.

Robinson, A.R., Golnaraghi, M., Leslie, W.G., Artegiani, A., Hecht, A., Lazzoni, E., Michelato, A., Sansone, E., Theocharis, A., Unluata, U., 1991. The eastern Mediterranean general circulation: features, structure and variability. Dynamics of Atmospheres and Oceans 15 (3–5), 215–240.

Robinson, A.R., Arango, H.G., Warn-Varnas, A., Leslie, W.G., Miller, A.J., Haley, P.J., Lozano, C.J., 1996. Real-time regional forecasting. In: Malanotte-Rizzoli, P. (Ed.), Modern Approaches to Data Assimilation in Ocean Modelling, Elsevier Oceanography Series, Elsevier Science, The Netherlands. pp. 377–412.

Sellschopp, J., 1997. A towed CTD chain for two dimensional high resolution hydrography. Deep-Sea Research 44, 147–165.

Sellschopp, J., Robinson, A.R., 1997. Definition and forecasting of ocean conditions during rapid response. Proc. Int. Conf. Rapid Environmental Assessment, Lerici, Italy, Mar. 10–14, 1997.

Theocharis, A., Georgopolous, D., Lascaratos, A., Nittis, K., 1993. Water masses and circulation in the central region of the eastern Mediterranean: eastern Ionian, south Aegean and northwest Levantine, 1986–1987. Deep Sea Research II 40 (6), 1121–1142.